https://doi.org/10.5194/egusphere-2022-395
Preprint. Discussion started: 25 May 2022

Holocene wildfire and vegetation dynamics in Central Yakutia, Siberia, reconstructed from lake-sediment proxies

Ramesh Glückler[1,4], Rongwei Geng[1,2,3], Lennart Grimm[1], Izabella Baisheva[1,4,6], Ulrike Herzschuh[1,4,5], Kathleen R. Stoof-Leichsenring[1], Stefan Kruse[1], Andrei Andreev[1], Luidmila Pestryakova[6], Elisabeth Dietze[1,7]

[1]Polar Terrestrial Environmental Systems, Alfred Wegener Institute Helmholtz Centre for Polar and Marine Research, Potsdam, Germany
[2]Key Laboratory of Land Surface Pattern and Simulation, Institute of Geographical Sciences and Natural Resources Research, Chinese Academy of Sciences, Beijing, China
[3]University of Chinese Academy of Sciences, Beijing, China
[4]Institute for Environmental Science and Geography, University of Potsdam, Potsdam, Germany
[5]Institute for Biochemistry and Biology, University of Potsdam, Potsdam, Germany
[6]Institute of Natural Sciences, North-Eastern Federal University of Yakutsk, Yakutsk, Russia
[7]Organic Geochemistry, German Research Centre for Geoscience (GFZ), Potsdam, Germany

Correspondence to: Ramesh Glückler (ramesh.glueckler@awi.de) and Elisabeth Dietze (elisabeth.dietze@awi.de)

Abstract. Wildfires play an essential role in the ecology of boreal forests. In eastern Siberia, fire activity has been increasing in recent years, challenging the livelihoods of local communities. Intensifying fire regimes also increase disturbance pressure on the boreal forests, which currently protect the permafrost beneath from accelerated degradation. However, long-term relationships between changes in fire regime and forest structure remain largely unknown. We assess past fire-vegetation feedbacks using sedimentary proxy records from Lake Satagay, Central Yakutia, Siberia, covering the past c. 10,800 years. Results from macroscopic and microscopic charcoal analyses indicate high amounts of burnt biomass during the Early Holocene, and that the present-day, low-severity surface fire regime has been in place since c. 4500 years before present. A pollen-based quantitative reconstruction of vegetation cover and a terrestrial plant record based on sedimentary ancient DNA metabarcoding suggest a pronounced shift in forest structure towards the Late Holocene. Whereas the Early Holocene was characterized by postglacial open larch-birch woodlands, forest structure changed towards the modern, mixed larch-dominated closed-canopy forest during the Mid-Holocene. We propose a potential relationship between open woodlands and high amounts of burnt biomass, as well as a mediating effect of dense larch forest on the climate-driven intensification of fire regimes. Considering the anticipated increase in forest disturbances (droughts, insect invasions, wildfires), higher tree mortality may force the modern state of the forest to shift towards an open woodland state comparable to the Early Holocene. Such a shift in forest structure may result in a positive feedback on currently intensifying wildfires. These new long-term data improve our understanding of millennial-scale fire regime changes and their relationships to changes of vegetation in Central Yakutia, where the local population is already being confronted with intensifying wildfire seasons.

https://doi.org/10.5194/egusphere-2022-395
Preprint. Discussion started: 25 May 2022

1. Introduction

Boreal ecosystems are facing increasingly severe wildfire seasons in recent years (Köster et al., 2021; Walker et al., 2019). In Yakutia (eastern Siberia) wildfire-related carbon emissions in the year 2021 surpassed those of 2020, which had already set a new record since the beginning of systematic satellite observations (Ponomarev et al., 2021; Voiland, 2021). Large areas were affected by the fires, leading to a partial breakdown of critical infrastructure and covering cities with harmful smoke for weeks. Furthermore, overwintering fires, smoldering in peatlands even during Yakutia's extreme winters, can contribute substantially to the region's burnt area in subsequent fire seasons (Xu et al., 2022). Central Yakutia is now among the most fire-prone regions of eastern Siberia and the whole boreal zone (Kirillina et al., 2020).

Eastern Siberia, and the Republic of Sakha (Yakutia) as its largest administrative unit, is unique among the boreal biomes, with deep permafrost and larch-dominated, deciduous forests (Deluca and Boisvenue, 2012; Rogers et al., 2015). These forests provide valuable ecosystem services both for the local communities and on continental to global scales, for example, by protecting carbon-rich permafrost from accelerated degradation (Kukavskaya et al., 2013; Herzschuh et al.; 2016; Herzschuh, 2020; Holloway et al., 2020; Stuenzi et al., 2021). Next to weather extremes or insect invasions, wildfires are the most important ecological disturbance in this region (Tei et al., 2019; Kharuk et al., 2021). The current fire regime of Siberia – generally described as consisting of mostly low-intensity surface fires when compared to the boreal zone of North America (Rogers et al., 2015) – has already been observed to intensify with increasing temperatures (Ponomarev et al., 2018). Simultaneously, a prolonged snow-free period (Bulygina et al., 2009) can increase fire probability in months that were previously not associated with the annual fire season. It has been suggested that continued global warming and its direct and indirect consequences will lead to increased tree mortality and changes in species composition (Kukavskaya et al., 2013; Shuman et al., 2017; Tei et al., 2019). Due to a complex network of environmental feedbacks, impacts of these changing fire regimes on the structure of the vast eastern Siberian larch forests are yet to be well understood, especially on longer timescales. Considering the slow growth rates of trees in the extreme continental conditions of Central Yakutia and the time-lagged adaptation of forests to climatic changes (Kruse et al., 2016), long-term studies are especially important to obtain a full picture of fire-vegetation interactions.

Central Yakutia is covered with a great number and variety of lake systems. Although their sediment bodies are promising long-term archives of past environmental processes and conditions, few studies have systematically analyzed fire proxies such as macroscopic charcoal in the lakes of this region. In a study of sediment cores from two lakes close to the republic's capital Yakutsk, high charcoal accumulation in the Early Holocene (10,000 years before present; yrs BP) coincided with an open larch forest (Katamura et al., 2009a). During the Mid-Holocene, after 6000 yrs BP, the pollen record indicates a rapid spread of *Pinus*, while charcoal accumulation decreases to very low levels. However, the authors suggest that the Early Holocene part of their sediment core may have been influenced by erosional input, and thus come to conclude that there is no significant relationship between fire and vegetation. A similar conclusion has been drawn by Katamura et al. (2009b), suggesting that a Holocene charcoal record from a thermokarst lake on the Lena-Aldan fluvial terrace is indicative of redeposition during lake

https://doi.org/10.5194/egusphere-2022-395
Preprint. Discussion started: 25 May 2022

development rather than a direct result of wildfire activity. Glückler et al. (2021) have recently contributed a high-resolution charcoal record from an intermontane basin lake in southwestern Yakutia, covering the last two millennia, and compared it to reconstructed vegetation, climate, and phases of human expansion. However, since the modern regional vegetation composition was already established and remained similar during much of the Late Holocene, no clear impacts of vegetation changes on wildfire activity or vice-versa were found.

Of these few studies containing long-term fire reconstructions in Yakutia, none report clear relationships between changes in fire regime and vegetation composition. Considering the strong dependence of fire regimes on their fuel source (Rogers et al., 2015; Archibald et al., 2018) and the major changes of vegetation structure that occurred during the Holocene and earlier warm periods (Andreev et al., 1997; Velichko et al., 1997; Dietze et al., 2020; Courtin et al., 2021), this seems surprising. Studies from other regions of the Russian boreal, however, point towards various potential feedbacks between fire and vegetation. During past interglacials in Chukotka, boreal forest dominated by larch has been generally related with low-intensity biomass burning (Dietze et al., 2020). At the southern edge of Lake Baikal, Barhoumi et al. (2021) find a severe fire regime from c. 11,000–6500 yrs BP, related to dark taiga vegetation (*Pinus sibirica*, *Abies sibirica*, *Picea obovata*), before the onset of the present-day surface fire regime, coinciding with a shift towards light taiga (*Pinus sylvestris*, *Betula* sp.). Feurdean et al. (2021[Accepted]) report how frequent high-severity fires could lead to changes in forest structure and composition in the Tomsk region (western Siberia). High fire activity coincided with a low peatland water level and intermediate forest density, and it occurred in both light and dark taiga. In the northern Ural region, Barhoumi et al. (2020) report predominantly climate-driven vegetation dynamics in the Early Holocene due to lower reconstructed fire activity, whereas in the Late Holocene increasing fire activity might have driven a vegetation shift from dark to light taiga. However, the limited number of long-term fire-vegetation studies set in Central Yakutia prevents an evaluation of fire-vegetation feedbacks in this important region.

The main objective of this study is to identify long-term relationships between changing fire regimes and boreal forest structure in Central Yakutia, and to discuss potential future trajectories in a warming climate. We do this by reconstructing (I) long-term wildfire history, derived from a new, continuous record of sedimentary macroscopic charcoal from a thermokarst lake, and comparing it to (II) the history of vegetation composition with a REVEALS-transformed pollen record and data on sedimentary ancient DNA of terrestrial plants.

2. Methods

2.1 Location

Lake Satagay (N 63.078, E 117.998; 114 m a.s.l.) is situated in the Nyurbinsky District of the western part of the Central Yakutian Lowlands, 600 km west of the republic's capital Yakutsk (Fig. 1). It lies in the vicinity of the Vilyuy River (20 km), a western tributary to the Lena River. Surrounded by flat topography and other thermokarst lakes, Lake Satagay covers an area of 1.7 km² with a maximum water depth of 1.8 m. The region around the lake is underlain by Jurassic sandstone, covered by alluvial and lacustrine Quaternary sediments (Ministry for Natural Resources and Ecology of the Russian Federation, 2012,

https://doi.org/10.5194/egusphere-2022-395
Preprint. Discussion started: 25 May 2022

2014). The area is directly accessible via the Vilyuy Highway (5 km) through forest trails. Apart from smaller settlements, the closest larger town is Nyurba with a population of c. 10,000 people (30 km). The lakes in this region and their surrounding grasslands ("alaas" landforms) have traditionally been used for agriculture (e.g. hay-making; Crate et al., 2017).

Drowning meadows near the shoreline, a flat bathymetry, and shallow water depth make Lake Satagay a typical late-stage thermokarst lake: it is mostly groundwater dominated and was most likely initially created by local ice-rich permafrost degradation. The resulting water-collecting depression subsequently expanded over time while partially filling up with organic-rich deposits to eventually form the present-day thermokarst lake (Boike et al., 2016; Crate et al., 2017). Long-term development of the lake is analyzed in more detail by Baisheva et al. (2022[In prep.]).

Present-day vegetation around the lake, as recorded during fieldwork in 2018 (Kruse et al., 2019) and observed by remote sensing vegetation classification (Geng et al., 2022[Accepted]; see Fig. 1), is dominated by dense, closed-canopy *Larix gmelinii* (Gmelin larch) tree stands. In between, there are occasional mixed, open-canopy stands of *Larix* together with *Picea obovata* (Siberian spruce), *Pinus sylvestris* (Scots pine), and less often *Betula pendula* (silver birch). Ground vegetation close to the lake consists primarily of mosses in addition to some lichens and grasses. Plenty of deadwood can be found, indicating disturbances to the forest (Kruse et al., 2019).

Central Yakutia is known for its extremely continental climate and the resulting large annual temperature range, having reached record values of around -70°C in winter and almost 40°C in summer. Based on CRU TS v.4.03 interpolated observational climate data (Harris et al., 2020) for the reference period of 1961 to 1990 at Lake Satagay, mean January temperature is -35°C, whereas mean July temperature is 17°C. Precipitation is very low during winter, most of the mean annual sum of 280 mm occurs during the warmer summer months (June-August).

The larger region around Lake Satagay and the Central Yakutian Lowlands in general, especially west of the Lena River, has been struck by record wildfires in recent years. Data from the MODIS Terra and Aqua satellites combined burned area product (MCD64A1 Version 6; Giglio et al., 2016), obtained for a 100 km buffer around Lake Satagay, shows that four of the five years with the largest burned area occurred only recently in the 20+ years timespan of available data (in decreasing order: 2021, 2014, 2019, 2002, 2018; Fig. 2b). An explorative application of the well-established Canadian Forest Fire Danger Rating System (Stocks et al., 1989), a fire weather index (FWI) derived from daily ERA5 climate reanalysis data (Hersbach et al., 2020) at Lake Satagay for the last 70 years, independently displays an increasing trend of climate-induced wildfire probability in the summer months starting around 2010 (Fig. 2a). It is likely that the current fire regime will continue to intensify with warming temperatures, as suggested also by a high positive correlation between observed burnt area and calculated summer FWI (Fig 2c).

2.2 Fieldwork and subsampling scheme

Fieldwork at Lake Satagay was conducted in August 2018 (Kruse et al., 2019). Sediment core EN18224-4 was obtained with a hammer-modified UWITEC gravity corer from the deepest region of the lake, at a water depth of 1.8 m based on point measurements with a Hondex PS-7 ultrasonic depth sounder. The 121-cm-long sediment core was sealed in its PVC tube, cut

https://doi.org/10.5194/egusphere-2022-395
Preprint. Discussion started: 25 May 2022

into two segments (0–100 cm and 100–121 cm), and subsequently transported to Germany in a cooled thermobox to be stored at the Alfred Wegener Institute (AWI) Potsdam at 4°C. After opening the sediment core, subsampling was done in October 2020 to obtain a continuous sequence of 111 sediment samples for charcoal analysis (1 cm^3), 48 of which were also used for the extraction of the pollen fraction. Additionally, 61 samples (2 cm^3) were extracted for the analysis of sedimentary ancient DNA (sedaDNA), while ten bulk sediment samples for dating were taken, spread equally across the core at every c. 10 cm.

2.3 Core dating

Bulk samples were freeze-dried and homogenized in a planetary mill before being sent to AWI Bremerhaven for AMS radiocarbon dating at the MICADAS laboratory, following standard protocols (Mollenhauer et al., 2021). Resulting ^{14}C ages were calibrated using the IntCal20 calibration curve (Reimer et al., 2020) in R (v.4.0.2; R Core Team, 2020) during age-depth modeling with Bacon (v.2.5.7, R package "rbacon"; Blaauw et al., 2021; Blaauw and Christen, 2011).

2.4 Charcoal and pollen extraction

To assess direct relationships between fire and vegetation composition, the same sediment sample was separated into a macroscopic charcoal and a pollen fraction following Glückler et al. (2021). In short, sediment samples were disaggregated by soaking in sodium pyrophosphate ($Na_4P_2O_7$) overnight. They were then infused with marker spores from *Lycopodium clavatum* tablets (Department of Geology, Lund University) that were dissolved in 10% hydrochloric acid (HCl). All samples were wet-sieved at 150 µm mesh width. The larger fraction, containing the macroscopic charcoal particles, was bleached with <5% sodium hypochlorite (NaClO) to improve distinction between charcoal and other dark organic particles. The smaller fraction, containing the pollen grains and non-pollen palynomorphs, was subsequently reassembled by multiple rounds of centrifuging, decanting, and adding of the remaining suspension. After this step, preparation of 48 pollen samples followed the standard protocols of Andreev et al. (2012).

Macroscopic charcoal samples were counted under a Zeiss Stemi SV 11 Apo stereomicroscope. Black, opaque charred particles were quantified and categorized according to size classes, from 150–300 µm (small), 300–500 µm (medium) to >500 µm (large), and their morphology, following the charcoal morphotype identification scheme established by Enache and Cumming (2007). Charcoal morphotypes were grouped into three higher level categories of angular, elongated, or irregular shapes. Ten samples were counted a second time to derive a mean counting error. Pollen grains and non-pollen palynomorphs were identified on glass slides under a Zeiss Axioskop 2 microscope at 400x magnification. *Lycopodium* marker spores and pollen were counted until a total of at least 300 terrestrial pollen grains was reached. In 12 pollen samples, at every c. 10 cm of the sediment core, microscopic charcoal particles were counted to a total of at least 300 (sum of microscopic charcoal and *Lycopodium* spores; Finsinger and Tinner, 2005).

https://doi.org/10.5194/egusphere-2022-395
Preprint. Discussion started: 25 May 2022

2.5 Sedimentary ancient DNA (sedaDNA) approach

The preparation of 61 samples for evaluation of sedaDNA is outlined in detail in Baisheva et al. (2022[In prep.]). In short, DNA was extracted from sediment samples using a Qiagen Power Soil isolation kit before being concentrated with a GeneJET PCR purification kit. PCR amplification of plant DNA was done by using the well-established universal plant primers targeting a short fragment of the trnL P6 loop on the chloroplast genome (Taberlet et al., 2007) modified with a unique NNN-8bp tag on each primer to establish sample separation. Pooled PCR products were then sequenced in paired-end mode using an Illumina NextSeq 500 sequencing device at Gensupport. Sequencing raw data was analyzed with Obitools (Boyer et al. 2017) and taxonomic classifications were based on matches against the Arctic and boreal vascular plant database (Sønstebø et al., 2010; Willerslev et al., 2014; Soininen et al., 2015). After removal of aquatic plants from the dataset, all identified terrestrial plant types with a total abundance of >0.1% at their highest taxonomical level were used for visualization, indicating the presence or absence of individual plant types within the sedaDNA.

2.6 Statistical methods

From the charcoal concentration per sample (particles cm^{-3}), a charcoal accumulation rate (CHAR, particles cm^{-2} yr^{-1}), interpolated to median temporal resolution, was calculated using the R script presented in Glückler et al. (2021). The background component of charcoal accumulation, indicative of the overall trends in the amount of biomass burned (Higuera et al., 2007), was determined by locally estimated scatterplot smoothing (LOESS) in a moving window of 25% of the record. Because of the low temporal resolution of the record of 100 ± 43 years (mean ± 1σ), the complementary peak component, often used to identify individual fire episodes, was not determined. Apart from this "classic" charcoal decomposition approach, we also included the alternative "robust" method, where additional uncertainties from charcoal counting, dating, as well as specific user input choices (i.e. smoothing window width) are integrated through Monte-Carlo-based random sampling (Dietze et al., 2019).

The pollen percentage data were transformed via the REVEALS method (Sugita, 2007) to estimate the past relative vegetation cover (R package "DISQOVER"; Theuerkauf et al., 2016), using relative pollen productivity and dispersal estimates of a harmonized dataset for the Northern Hemisphere extratropic zone (Wieczorek and Herzschuh, 2020). All pollen types with a total cumulative coverage across all samples exceeding 0.1% were used for visualization. To evaluate potential relationships between vegetation cover and charcoal counts, both datasets were centered log-ratio transformed (R package "compositions"; van den Boogaart et al., 2021) and used for principal component analysis (PCA; R package "vegan", Oksanen et al., 2020). For correlations, a Pearson correlation coefficient was calculated.

Unique zones within the charcoal, pollen, and sedaDNA distributions were identified with stratigraphically constrained cluster analysis (Grimm, 1987; using the R packages "vegan" and "rioja"; Juggins, 2020). Only a significant number of zones, according to comparison with a broken-stick model, is visualized (Bennett, 1996).

https://doi.org/10.5194/egusphere-2022-395
Preprint. Discussion started: 25 May 2022

3. Results

3.1 Chronology

Sediment core EN18224-4 displays a mostly homogenous texture with dark-brown colors from organic-rich deposits, lacking any lamination. A detailed description of the core sediment facies can be found in Baisheva et al. (2022[In prep.]). Bulk sediment ^{14}C dating shows a well-ordered sequence of dating points without age reversals (Table 1). The surface sample, dating back to 1345.5 ± 36.5 cal. yrs BP (mean ± 2σ), shows a clear age offset. Such surface age offsets often occur in lakes of eastern Siberia (e.g. Colman et al., 1996; Vyse et al., 2020; Glückler et al., 2021) and can have a variety of causes. In the present shallow lake, the flat surrounding topography and the lack of a major inflow limit the ability of surface runoff, thermokarst slumping, or fluvial input to deposit old organic carbon from eroded permafrost compared to other lakes (Glückler et al., 2021). Similarly, the lack of nearby carbonaceous rock formations excludes the presence of a hardwater effect (Philippsen, 2013). Therefore, the age-offset is most likely a consequence of older sediment mixing with recent deposits in the uppermost part (Biskaborn et al., 2012). The surface ^{14}C age was therefore not included in the age-depth modeling. Instead, a recent age was assumed (i.e. year of core extraction, 2018 CE). The resulting chronology suggests a basal age of the sediment core of c. 10,800 cal. yrs BP, covering most of the Holocene (Fig. 3a; for the original Bacon chronology see Supplementary Figure 1). The dating uncertainty, i.e. the 2σ range of all age-depth models included in the chronology, is on average 601 ± 279 yrs (mean ± 1σ). For all following analyses and figures the median age values are used. According to those, mean sedimentation rate is 0.14 ± 0.09 mm yr^{-1}, with higher rates of up to 0.42 mm yr^{-1} between c. 37 and 56 cm (Fig. 3b). This chronology is further reinforced by a pronounced expansion of pine trees, clearly visible in the pollen record at c. 5400 cal. yrs BP. The timing of this expansion fits within the range reported by previous studies in the region (e.g. Müller et al., 2009; Andreev and Tarasov, 2013).

3.2 Charcoal

In 111 samples continuously covering the sediment core, a total of 4206 macroscopic charcoal particles was identified, resulting in a mean of c. 38 particles per cm^3 (Fig. 3c) or a mean charcoal accumulation rate (CHAR) of 0.38 ± 0.5 particles cm^{-2} yr^{-1} (mean ± 1σ, Fig. 7b). The median temporal resolution of all charcoal samples is 100 ± 43 years. Charcoal accumulation varies in three major phases throughout the Holocene with highest CHAR in the Early Holocene, intermediate CHAR in the Mid-Holocene, and low CHAR during the Late Holocene until present day. Most prominently, CHAR shows a distinct peak around 9600 yrs BP, reaching a record-wide maximum of 2.58 particles cm^{-2} yr^{-1}. The mean CHAR of the Early Holocene (c. 10,800 to 8500 yrs BP) is 1.0 ± 0.73 particles cm^{-2} yr^{-1}. After that, it decreases to lower intermediate levels until c. 4500 yrs BP (0.29 ± 0.17 particles cm^{-2} yr^{-1}). From there until present day, CHAR remains at low levels (0.09 ± 0.06 particles cm^{-2} yr^{-1}). Robust CHAR, with its added uncertainties from a random sampling approach, mirrors the described trends and closely overlaps with the smoothed background component of classic CHAR. The low-resolution microscopic charcoal shows a very similar trend to the macroscopic charcoal concentration (Fig. 3c), with a distinct maximum at 9800 yrs BP (100 × 10^3 particles

https://doi.org/10.5194/egusphere-2022-395
Preprint. Discussion started: 25 May 2022

cm^{-3}), followed by intermediate levels until 5500 yrs BP (40 × 10^3 particles cm^{-3}), and low levels until present day (10 × 10^3 particles cm^{-3}).

Most macroscopic charcoal particles are rather small, with 50.2% belonging to the small size class (150–300 µm), whereas 27.1% and 22.7% are in the medium (300–500 µm) and large (>500 µm) size classes, respectively. By far the most particles demonstrate angular shapes (85%), with few contributing to either irregular (10.4%) or elongated (4.6%) morphotype classes. Cluster analysis of the charcoal sum and its three morphotype timeseries suggests three zones separated at 5300 and 9000 yrs BP, marking the three general phases of CHAR described above (Fig. 7b, c). The oldest zone, characterized by the record's highest CHAR values, is dominated by higher shares of large particles and a high abundance of angular morphotypes at 80–90%. The most recent zone shows low CHAR coinciding with decreasing shares of large and angular types, and an increase of irregular types to 30–40%.

3.3 Pollen

REVEALS-transformed pollen data indicates that the vegetation around Lake Satagay was dominated by *Larix* throughout most of the past c. 10,800 years, with maximum cover of up to 70% around 5500 yrs BP and within the recent centuries (Fig. 4). In addition, *Betula*, *Picea*, and *Pinus* appear with high cover of up to 30%, while *Salix* (willow), *Abies* (fir), *Alnus* (alder), and Cupressaceae (cypress) mostly stay below 10%. Non-arboreal pollen (NAP) are dominated by Poaceae and Cyperaceae. Other NAP found are Asteraceae, *Thalictrum*, Rosaceae, and small numbers of *Artemisia*, Ericales, Fabaceae, Onagraceae, and Caryophyllaceae. The original pollen counts also feature a high number of algae in the lowest segment of the core (10,800–7000 yrs BP), and some Polypodiaceae spores in the upper part of the core (5400–2000 yrs BP; Supplementary Figure 2).

Compared to the original, non-transformed pollen record, the REVEALS-transformed, quantitative vegetation reconstruction greatly increases relative shares of *Larix*. The reason for this difference is an underrepresentation of *Larix* in pollen assemblages compared with other arboreal taxa such as *Pinus*, caused by the relatively low pollen production and pollen dispersal range of larch trees (Edwards et al., 2000; Cao et al., 2019b). Trends observed in the original pollen record are well captured by the REVEALS-transformed data. Because of that and the correction of species-specific taphonomy, only the REVEALS data will be discussed in more detail.

Cluster analysis separates the quantitative vegetation reconstruction into two major zones: the lower zone (10,800–7000 yrs BP) is characterized by a high cover of Poaceae and arboreal pollen dominated by *Larix* and *Betula*. The upper zone (7000 yrs BP–present), on the contrary, displays a mixed forest that is clearly dominated by *Larix*. *Betula* decreases and Poaceae have been giving way to a higher cover of Cyperaceae. When interpolated to the same sample age intervals as the macroscopic charcoal accumulation rate, cluster analysis identifies additional zones, including a separation at 5400 yrs BP (Fig. 7d). At this time, pine trees rapidly extend their cover, while *Salix* is only seen on a few occasions from there on. The original pollen counts (Supplementary Figure 2) demonstrate similar trends. There, cluster analysis also identifies a zone at 5400 yrs BP, when *Betula* pollen give way to quickly increasing numbers of *Pinus* pollen.

https://doi.org/10.5194/egusphere-2022-395
Preprint. Discussion started: 25 May 2022

The PCA for transformed pollen types clearly distinguishes Early from Late Holocene samples along principal component 1 (PC1), explaining 23.7% of the dataset variability (Fig. 8a). As indicated by the opposing vectors, PC1 describes two major states of forest structure present in the reconstruction, with open larch-birch woodlands in the Early Holocene (negative values of PC1), opposed to a denser, larch-dominated forest in the Late Holocene (positive values of PC1). PC1 is negatively correlated with charcoal concentration (r = -0.71, r^2 = 0.51, $p < 0.001$), i.e. the dense forest state of PC1 coincides with low charcoal concentration, whereas the open woodland state coincides with high charcoal concentration (Fig 8b).

3.4 Sedimentary ancient DNA

Analysis of sedaDNA revealed 79 DNA sequence types of terrestrial plants identified to different taxonomic levels, which were then collapsed to family level, resulting in 28 different plant families (Fig. 5). With cluster analysis, four zones are identified within the sedaDNA proxy, in agreement with pollen and charcoal zones. The first zone (10,800–9300 yrs BP) comprises *Betula*, Saliceae, and *Populus*, together with a great variety of flowering plants and grasses (Asteraceae, Chenopodiaceae, Onagraceae, Rosaceae, Poaceae, Urticaceae). The Onagraceae here include *Chamaenerion angustifolium* (fireweed). The second zone (9300–5400 yrs BP) continues with similar identified trees, including now more *Larix*, while for non-arboreal plants most samples now have reads from Poaceae and Asteraceae. In the next zone (5400–3800 yrs BP), *Betula* is identified in fewer samples than before, giving way to *Larix*, Saliceae, and some *Picea*. Compared to previous zones, fewer non-arboreal plants have been identified here. In the most recent zone (3800 yrs BP–present) samples show reads from various tree tribes and genera (*Betula*, *Alnus*, *Larix*, Saliceae), while no more *Picea* or *Populus* are identified. Fewer samples than in previous zones show reads from Poaceae, whereas Cyperaceae are more common. Asteraceae are present in most samples.

4. Discussion

4.1 Reconstructed wildfire activity

Charcoal analysis suggests a pronounced shift in the fire regime around Lake Satagay in the Early Holocene (c. 9000 yrs BP) and until the Mid-Holocene (c. 5300 yrs BP). We suggest that the high CHAR during the Early Holocene represents a high-severity fire regime (in the sense that all aggregated wildfires were able to burn large amounts of biomass, not necessarily that individual fires were of high severity), whereas low CHAR since the Mid-Holocene indicates the establishment of the present-day low-severity surface fire regime around Lake Satagay (Rogers et al., 2015). Following definitions in Keeley (2009), “fire severity” here describes the amount of above- and belowground biomass consumed by a fire, which is represented by the overall amounts of charcoal deposited in a lake, whereas “fire intensity” is a measure of energy output. High fire intensities generally lead to a higher fire severity with different impacts on forest vegetation and recovery compared to low intensity fires (Rogers et al., 2015).

A high abundance of charcoal in lake sediments suggests increased amounts of biomass burned, due to larger burnt areas per fire, more intense fires, more frequent fires, or a mixture of all three aspects. Although the temporal resolution of the charcoal

https://doi.org/10.5194/egusphere-2022-395
Preprint. Discussion started: 25 May 2022

record is too low to apply the common peak detection method to screen for individual fire events (Whitlock and Larsen, 2001), the CHAR background component still suggests a change from high to low amounts of biomass burned during the Mid-Holocene (Fig. 7b; Whitlock and Anderson, 2003). The increased share of large particles in the pronounced peak of CHAR around 9600 yrs BP points towards a higher fire intensity in the Early Holocene. High-intensity fires generally produce larger flames (Hood et al., 2018), enabling them to better scorch trees and thus produce larger and robust, block-like charcoal particles (Enache and Cumming 2006, 2007). In addition, high fire intensity enables larger charcoal particles to be injected higher into the atmosphere in stronger plumes (Ward and Hardy, 1991), which are then better conserved during deposition.

During low-severity fires, the canopy remains intact, and lower accompanying fire intensities usually do not lead to strong convection (Fig. 6). Both factors limit the plume injection height and subsequent spread of charcoal particles (Clark, 1988; Vachula and Richter, 2018), leading to lower CHAR in lake sediments. However, classical methods of using charcoal as a fire proxy do not currently allow for a quantitative evaluation of fire intensity, specifically. Additional methods would need to be applied to quantify thermal energy output during charcoal production, such as using intensity-specific fire biomarkers (Ding et al., 2015; Nakane et al., 2017; Dietze et al., 2019; Dietze et al., 2020; Karp et al., 2020), analyzing the particles' degree of aromaticity with reflectance microscopy (Hudspith et al., 2015) or a scanning electron microscope enabled for energy dispersive X-ray analysis (SEM-EDX; Reza et al., 2020), or Fourier transform infrared spectroscopy (FTIR; Maezumi et al., 2021).

During the fire regime shift around Lake Satagay, we also find a shift from more angular to more irregular charcoal morphotypes, indicative of changing fuel types. Connecting charcoal morphotypes with fuel types is an ongoing challenge, with different approaches and interpretations among the various experimental and applied studies. Enache and Cumming (2006) describe angular morphotypes as most likely originating from woody biomass. However, both angular and irregularly shaped morphotypes have also been shown to resemble charred grass biomass, resulting in flat sheets with a visible epidermal cell structure (Jensen et al., 2007; Mustaphi and Pisaric, 2014). Elongated particles are suggested to result from burnt grasses (Enache and Cumming, 2006; Feurdean, 2021), conifer needles (Mustaphi and Pisaric, 2014), or from breakage of other particles (Enache and Cumming, 2007). Further potential main fuel sources could be fern and shrub leaves, which are categorized as either angular or irregular, and resins, which form irregular, glassy shapes without visible structure (Jensen et al., 2007). Based on comparisons with those previous studies, we suggest a predominantly woody origin for the block-like, angular morphotypes at our study site. Grasses are more likely represented by irregular or elongated particles because of their fragility and clearly visible, often frayed, cellular structure. Therefore, higher shares of woody morphotypes at Lake Satagay might indicate that, in the Early Holocene, a potentially more severe and intense fire regime enabled the thorough combustion of tree biomass. In contrast, low-severity surface fires can explain the increasing shares of predominantly grassy and more fragile morphotypes in the Late Holocene. Charring experiments with local vegetation samples can help to assign charcoal morphologies to fuel types more precisely (Vachula et al., 2021).

We assume that charcoal in the Early Holocene has been deposited directly by fires after atmospheric transport, in contrast to the suggestion of resulting from erosion by Katamura et al. (2009ab) for similar lake systems in Central Yakutia. There, the

https://doi.org/10.5194/egusphere-2022-395
Preprint. Discussion started: 25 May 2022

authors found trends in CHAR and pollen distributions that very closely match the results of this study. However, they argue that high Early Holocene charcoal accumulation was caused by early internal lake sedimentation processes during thermokarst lake formation instead of direct deposition following fires. We consider secondary charcoal transport as unlikely because the flat topography around Lake Satagay limits surface runoff and secondary deposition. Also, during the fieldwork, no signs of thaw slumping along the reed-covered lake shore were found. In addition, the pollen record suggests that the lake already existed at 10,800 yrs BP (high counts of algal palynomorphs even in its deepest samples; see Supplementary Figure 2). This is reinforced by the presence of diatoms and aquatic, submerged plants (Potamogetonaceae), revealed by sedaDNA within the lowest samples of the sediment core (Baisheva et al., 2022[In prep.]). Therefore, initial lake development of Lake Satagay probably occurred a few millennia before the earliest temporal coverage of our sediment core (i.e., before 10,800 yrs BP; Baisheva et al., 2022[In prep.]). For these reasons, we suggest that charcoal particles were mainly transported through the air and resemble trends of biomass burning around the lake.

Microscopic charcoal counts (Fig. 3c) independently support the trends observed for the larger particles. Additionally, they suggest that the Holocene change in wildfire regime may not only have occurred locally at this lake, but also on a broader scale. This is because microscopic particles can stay airborne longer and thus be transported further, effectively incorporating signals from a larger source area compared to macroscopic particles (Whitlock and Larsen, 2001).

The recent fire regime intensification, as seen in the last decade of observational data (Fig. 1), is not reproduced in the charcoal record. Most likely, the present thermokarst lake system records changes in fire regimes with a certain time-lag, i.e. the time from the first visible changes in wildfire appearance (c. 2010 CE) to the actual change in sedimentary charcoal deposition may be longer than what is covered by our sediment core obtained in 2018 CE. Furthermore, the topmost millimeters/centimeters of a sediment core, corresponding to the most recent environmental history, are often difficult to interpret due to high water content, active sediment mixing processes, and/or compaction during sediment core retrieval (Glew et al., 2001). In addition, CHAR heavily depends on the sedimentation rate derived from age-depth modeling. In this study, there is a sediment-mixing-based radiocarbon age offset in the surface sediment. Although the chronology is thought to be robust and is independently supported by the results from pollen analysis, this age offset may introduce some uncertainty into the sedimentation rate of the topmost core centimeters. For these reasons, the topmost sample of the charcoal record is not expected to show the most recent changes in fire regime.

Recently, Constantine and Mooney (2021) found that the use of sodium hypochlorite for bleaching organic excess material in macroscopic charcoal samples can lead to a loss of charcoal particles from low-intensity fires (<400°C). In a region like eastern Siberia, where a comparably low-intensity surface fire regime is expected, this may lead to a variable degree of underestimation of low-intensity fire activity depending on changes in fire regime attributes through time. However, at Lake Satagay the non-bleached microscopic charcoal independently mirrors trends of macroscopic charcoal, suggesting that the general trends discussed in this study are well captured. During the preparation of pollen slides, microscopic charcoal is instead exposed to other chemicals such as potassium hydroxide. Comparative studies with bleached and non-bleached sedimentary samples, as

https://doi.org/10.5194/egusphere-2022-395
Preprint. Discussion started: 25 May 2022

well as potential alternative methods of bleaching or particle quantification, may be useful to safely exclude any bias against low-intensity fires and further develop charcoal as a paleoenvironmental proxy.

4.2 Reconstructed vegetation composition

Both original pollen abundance and the REVEALS-transformed pollen record display a pronounced Mid-Holocene vegetation change from open larch-birch woodlands towards the modern, denser mixed larch forest. This is demonstrated by high proportions of *Betula* and Poaceae pollen in the Early Holocene (around 10,000 yrs BP), when few tree taxa, apart from those typical for the postglacial open woodlands in Yakutia, were present (Andreev et al., 1997; Katamura et al., 2006; Müller et al., 2009). Birch trees of this postglacial landscape are thought to have grown in a sparse, open forest at limited height (so-called "yornik"; Andreev et al., 1997). The ratio of deciduous to evergreen trees is exceptionally high during the Early Holocene compared to the rest of the record. The sudden expansion of *Pinus* after 5400 yrs BP, especially on patches of sandy substrate (see Fig. 1), is also a typical feature of Holocene vegetation dynamics in Yakutia and has been witnessed in many other paleoenvironmental studies (depending on study site and chronology it has been reported to occur between c. 7000 and 4000 yrs BP; Müller et al., 2009; Andreev and Tarasov, 2013; Tian et al., 2018; Cao et al., 2019ab). Since the timing of the pine tree expansion in this study falls right within the range of reported ages, it independently reinforces the suitability of the applied chronology.

After 5400 yrs BP a higher cover of Cyperaceae (e.g. *Carex*), graminoids, or sedges which are often found in marshes and wetlands, may indicate increased availability of wetland area around the lake, possibly due to decreasing water levels during late-stage thermokarst lake development (Baisheva et al., 2022[In prep.]). The non-transformed pollen record also shows fern spores (Polypodiaceae) after 5400 yrs BP. Ferns are typical understory vegetation, preferring shaded locations as found in a denser forest. *Salix*, prominent during the Early to Mid-Holocene, accompanies the earlier open woodland state of the forest, likely growing as an understory shrub in direct sunlight between scattered higher trees (Katamura et al., 2006; Müller et al., 2009).

The negative correlation of the REVEALS pollen PC1, indicative of forest density, with charcoal concentrations suggests that open woodlands may promote increased amounts of biomass burned, whereas a denser forest coincides with a lower severity fire regime. Other relationships of REVEALS pollen percentages with charcoal concentration suggest that a more severe fire regime occurs only once the ratio of AP/NAP falls below c. 4/1, corresponding to a tree cover of <80% (Supplementary Figure 3). Similarly, high charcoal concentrations occur when *Larix* cover is <50%, *Pinus* cover is <2.5% and/or *Betula* cover is >15%. Charcoal concentration and Poaceae cover display a high positive correlation, whereas charcoal and Cyperaceae are negatively correlated. High charcoal concentrations only occur when Cypeaceae, mainly growing on wetter sites, show a cover of <5%.

The sedaDNA data is in good agreement with the pollen-based vegetation reconstruction, but since DNA taphonomy pathways are more locally restricted, it sets a unique focus on vegetation close to the lake (Liu et al., 2020). In addition, it provides more detailed information with its higher taxonomic resolution. *Betula* and non-arboreal plant families are more prevalent in Early

https://doi.org/10.5194/egusphere-2022-395
Preprint. Discussion started: 25 May 2022

Holocene samples, including typical disturbance indicators such as *Chamaenerion angustifolium* (fireweed), which is known as a pioneer of freshly disturbed soils (Tsuyuzaki et al., 2018). At the same time, *Populus* was identified. These light-demanding, fast-growing aspen trees are also considered typical pioneering plants (Chytrý et al., 2008), linked to early stages of post-fire succession and pointing towards more frequent fire disturbances during the Early Holocene. Even though present in the pollen record, *Pinus* is noticeably absent in the sedaDNA data. There, the Pinaceae include only *Larix* and *Picea*. This is likely because *Pinus* tends to grow in isolated patches on dry, sandy soils at some distance from Lake Satagay (see Fig. 1), thus not contributing sufficiently to the locally derived sedaDNA record.

4.3 Fire-vegetation feedbacks on millennial timescales

Wildfires, vegetation, climate, and human activity are closely linked and can influence each other in many ways (Bowman et al., 2020). This makes it difficult to distinguish clear causal from purely statistical relationships in paleoenvironmental studies. At Lake Satagay, we find links between open larch-birch woodlands and a more severe fire regime (in the Early Holocene), as well as a denser, mixed larch-dominated forest coinciding with a less severe fire regime (in the Late Holocene). Furthermore, a high ratio of deciduous to evergreen trees coincides with more biomass burned (Fig. 7). Here, we discuss potential fire-vegetation feedbacks under varying climate and human activity throughout the Holocene that might explain these links.

Fire regimes in grasslands generally burn high amounts of biomass, as fires tend to be more frequent and move rapidly through a landscape of sufficient fuel conditions (Coffman et al., 2010; Archibald et al., 2013; Leys et al., 2017; Wragg et al., 2018). Reasons for this can be a higher susceptibility of open grasslands to drying in direct sunlight, together with well-combustible, fragile herb and shrub vegetation creating optimal, fine fuel conditions. An open forest structure also leads to increased wind speeds, accelerating fire spread and contributing to drying of ground vegetation. This directly applies to the often-thick ground vegetation of Central Yakutia, consisting of mosses, lichens, herbs, and shrubs (e.g. *Salix*, *Betula, Vaccinium*; Isaev et al., 2010; Kruse et al., 2019). Larch trees themselves are adapted to occasional surface fires and protected from extensive damage with a thick insulating bark (Wirth et al., 2005).

At Lake Satagay, the anthropogenic influence on the reconstructed fire and vegetation history is assumed to be low. Despite a continuous human presence throughout the Holocene, nomadic cultures living in Central Yakutia before c. 900 yrs BP are not assumed to have used fire on a wide scale. In recent centuries, the alaas landscape was used for agricultural purposes by the semi-nomadic Sakha people (Crate et al., 2017). Direct human impact on the fire regime likely increased only more recently, after the colonization of Yakutia by the Russians in the 16th and following industrialization in the 19th century (Glückler et al., 2021).

The climate, on the other hand, is an important environmental driver throughout the whole Holocene. Rising temperatures during the Late Glacial likely initiated widespread thermokarst processes after c. 14,000 yrs BP (Walter et al., 2007). The Holocene Climate Optimum in the Early to Mid-Holocene (c. 7000–5000 yrs BP; Ulrich et al., 2019) and subsequent cooling triggered vegetation change across Yakutia, including the rapid expansion of pine trees (Müller et al., 2009; Andreev and Tarasov, 2013), which is also evident in this study around 5400 yrs BP. Additionally, the Holocene Climate Optimum triggered

https://doi.org/10.5194/egusphere-2022-395
Preprint. Discussion started: 25 May 2022

the formation of new thermokarst lakes and wetlands, as well as the expansion of existing ones (Ulrich et al., 2019). This, together with a potential decrease of the lake water level, may have contributed to the increased sedimentation rate at Lake Satagay between c. 6000 and 5000 yrs BP (Fig. 3). Climate may be most relevant to wildfires by controlling the overall frequency of fire weather, i.e. the combination of dry, warm, and windy conditions and the length of the fire season. This leads to the question of whether rapid (i.e. within a few hundred years) climate-driven changes of vegetation composition resulted in adapted fire regimes, or if climatic change first drove fire regime changes that in turn supported a change in vegetation composition. As we lack vegetation-independent Holocene temperature and precipitation reconstructions for Central Yakutia, we can infer climate-driven fire regime changes only indirectly. Based on our cluster analyses, the separation between the Early Holocene high-severity fire and open woodland state and the intermediate fire and forest state of the Mid-Holocene occurs first in the transformed pollen record (9600 yrs BP), c. 600 years before the zone separation in CHAR (9000 yrs BP; Fig. 7). The separation of the Mid-Holocene intermediate and the modern conditions of the Late Holocene occurs almost at the same time in the transformed pollen record (5400 yrs BP) and CHAR (5300 yrs BP). However, although the charcoal morphotypes immediately mirror shifting vegetation composition at 5300 yrs BP, the total sum of CHAR decreases only c. 800 years later at c. 4500 yrs BP. In addition, trends of CHAR mirror the ratio of deciduous to evergreen trees, but with a time-lag of c. 500 years. Even though this time-lag is quite long, it might indicate that the fire regime shifts on long timescales occurred in response to the establishment of a new vegetative state. We suggest that Early to Mid-Holocene fire regime changes were driven by long-term vegetation changes, modified by short-term fire weather variations, until c. 4500 yrs BP. Once the modern, dense larch forest state was established, only climate remained as the main driver behind less pronounced fire regime changes on shorter, centennial timescales, eventually accompanied by anthropogenic fire use and management (Glückler et al., 2021).

With a fire regime burning high amounts of biomass in relation to open woodlands dominated by deciduous trees, this study adds a new case to the discussion of long-term fire-vegetation feedbacks in Siberia. It resembles some fire-vegetation dynamics found by Dietze et al. (2020) at Lake El'gygytgyn in Chukotka, where influxes of fire biomarkers (monosaccharide anhydrides, MAs) show a significant positive correlation with the presence of deciduous tree pollen (*Larix*, *Populus*, *Alnus*) in multiple past interglacials. In wetter periods, as indicated by abundant *Sphagnum* spores, fire activity is reduced. Evergreen *Picea* pollen, on the other hand, are not found to be related to the fire biomarker influx. However, increased tundra vegetation coincides with decreased MA influxes at Lake El'gygytgyn. MAs are a burn product of low-intensity fires (<350°C), whereas the macroscopic charcoal of this study is regarded mostly as a product of higher intensity fires (depending on fuel source c. 200–600°C; Conedera et al., 2009; Dietze et al., 2020). An application of both proxies would be needed for a better comparison, with the beneficial side effect of enabling the reconstruction of general fire intensity changes throughout time, using ratios of the two.

Fire seasons at Lake Satagay are becoming more severe since c. 2010 CE, concurrent with a trend of rising summer temperatures and decreasing precipitation (Fig. 2). Meanwhile, vegetation composition and cover are not suspected to have systematically changed during the last decade. Similarly, it is unlikely that a sudden shift in the share of human-caused fires

https://doi.org/10.5194/egusphere-2022-395
Preprint. Discussion started: 25 May 2022

occurred around 2010 CE. Even though the forest management system of Yakutia has undergone several adjustments in recent years (e.g. abstaining from extinguishing fires far from populated regions), a persistent shortage of funding exacerbated broad-scale suppression even before (Narita et al., 2021). With its close proximity to the Vilyuy highway, multiple settlements, and agriculturally used lands, these management changes are thus not assumed to have caused the most recent increase in burnt area. Together with the positive correlation of recently burnt area with the climate-derived fire weather index, this suggests that the recent fire regime intensification is driven mainly by the rapid change of climate.

Continued climate change is anticipated to lead to an increase of tree mortality as a consequence of more frequent droughts and insect invasions (Kukavskaya et al., 2013; Tei et al., 2019). While this may lead to younger tree populations or a shift in predominant species, it could also lead to an increased area of open woodlands within the coming decades to centuries, further supported by logging activities (Isaev et al., 2010; Kukavskaya et al., 2013). Considering such a potential "thinning trend" and a shift towards a more severe fire regime in open woodlands, comparable to the reconstructed Early Holocene state around Lake Satagay, this points towards a potential positive feedback on the currently intensifying fire regimes of Central Yakutia within the next decades to centuries.

Since an existing forest structure can adapt only slowly and is time-lagged to rapidly changing climatic conditions, the present-day dense larch forest might still be mediating the observed fire regime intensification. The ability of vegetation to mediate or amplify climate-driven fire regime changes and associated permafrost degradation has been discussed before (Higuera et al., 2009; Herzschuh et al., 2020). However, once the forest structure is pushed out of its current state (either directly, by slowly adapting to new climatic conditions, or indirectly, by increased mortality from disturbances) this mediating effect might eventually come to an end. If the fire regime regains a severity comparable to the Early Holocene, it may be able to sustain the newly developed open woodlands, stabilizing them as a new and markedly different state of boreal forest structure. Previous modeling studies support the hypothesis of two stable states of forest structure and the impact of changing fire regimes (Lasslop et al., 2016). Whether this "open woodland-fire feedback" is a likely scenario, and whether it could be mediated by a simultaneous degradation of ice-rich permafrost due to forest thinning that may lead to an increase in soil moisture and wetland areas (Fedorov et al., 2019; Ulrich et al., 2019; Stuenzi et al., 2021), presents an important research question for coupled fire-vegetation-permafrost modeling.

Future modeling studies that consider the open woodland-fire feedback are therefore needed to better constrain the probability of such a state change in Central Yakutia. Additionally, modeling could test whether a shift from the modern state towards the open woodland state would happen either gradually, as observed during the Early to Mid-Holocene, or display tipping-like state change behavior once the anthropogenically forced, intensifying fire regime surpasses a threshold in fire frequency, even on shorter timescales than what we can observe with paleoenvironmental studies (Lenton, 2012; Scheffer et al., 2012; Reyer et al., 2015).

https://doi.org/10.5194/egusphere-2022-395
Preprint. Discussion started: 25 May 2022

5. Conclusions

Through the analysis of sedimentary charcoal, pollen, and ancient plant DNA, fire and vegetation dynamics were reconstructed for the last c. 10,800 years at Lake Satagay. Results indicate that Early Holocene, open larch-birch woodlands were accompanied by high amounts of burnt biomass. From there, forest structure shifted towards the denser larch-dominated forest mixed with pine and spruce as observed today, which co-developed with a low-severity surface fire regime since c. 4500 yrs BP. Considering an anticipated increase in tree mortality, potentially leading to sparser tree populations, these results point towards a possible positive feedback on currently intensifying fire regimes in Central Yakutia. The presence of a dense larch forest might yet be mediating the true extent of the climate-induced fire regime intensification observed during the last decade. Ecological modeling should be able to test and better constrain this hypothesis, whereas spatially extended paleoenvironmental information could inform whether this suggested fire-vegetation feedback at Lake Satagay is only a local one, or whether it applies to regional or ecosystem-wide scales, also considering a diverse degree of human intervention in forest management. As local communities are already confronted with these changing environments and intensifying fire seasons, the urgency of understanding long-term and future pathways of fire-vegetation feedbacks only keeps growing.

Conflict of Interest

The authors declare that the research was conducted in the absence of any commercial or financial relationships that could be construed as a potential conflict of interest.

Author contributions

UH, SK and LP designed and lead the field works. RGl designed the sediment study supervised by ED and UH. RGl and KS subsampled the sediment core, RGl prepared the age dating process and created the chronology. RGe conducted the pollen analysis, supervised by AA and UH. LG conducted the charcoal-related laboratory work and analysis, supported by RGl and ED. IB and KS performed sedaDNA analyses. RGl wrote the initial version of the manuscript, supervised by ED. All authors commented on the initial manuscript.

Funding

This research has been supported by the European Research Council (grant no. Glacial Legacy: 772852), the Deutsche Forschungsgemeinschaft (DFG, German Research Foundation, grants no. DI 2544/1-1: #419058007 and 448651799), and the Russian Ministry of Education and Science (FSRG-2020-0019). Ramesh Glückler is funded by AWI INSPIRES (International Science Program for Integrative Research). Izabella Baisheva is funded by the German Academic Exchange Service e.V. (DAAD).

https://doi.org/10.5194/egusphere-2022-395
Preprint. Discussion started: 25 May 2022

Acknowledgements

Thanks to all members of the joint German-Russian expedition "Chukotka-Yakutia 2018". We thank Stuart Vyse and Paul Adam for supporting work on this study's sediment core. Philip Meister, Ingeborg Frommel, Rebecca Morawietz and Amelie Naderi kindly helped with subsampling the sediment core. We thank Thomas Böhmer and Peter Ewald for the transformation of the pollen data. Thanks to Cathy Jenks for help with English editing.

Data availability

The data presented in this study will be made publicly available via the PANGAEA database (https://pangaea.de; PANGAEA, 2022). The charcoal data will additionally be uploaded to the Global Paleofire Database (https://ipn.paleofire.org; International Paleofire Network, 2022). The sedaDNA metabarcoding data will be uploaded to the Dryad database (https://datadryad.org/; Dryad Digital Repository, 2022).

References

Andreev, A. A., Klimanov, V. A., and Sulerzhitsky, L. D. (1997). Younger Dryas pollen records from central and southern Yakutia. Quat. Int. 41–42, 111–117. doi: 10.1016/S1040-6182(96)00042-0.

Andreev, A. A., Morozova, E., Fedorov, G., Schirrmeister, L., Bobrov, A. A., Kienast, F., et al. (2012). Vegetation history of central Chukotka deduced from permafrost paleoenvironmental records of the El'gygytgyn Impact Crater. Clim. Past 8, 1287–1300. doi: https://doi.org/10.5194/cp-8-1287-2012.

Andreev, A., and Tarasov, P. (2013). "Northern Asia," in The Encyclopedia of Quaternary Science, 2nd Edition, Volume 4, eds. S. A. Elias and C. J. Mock (Elsevier) 164–172. doi: 10.13140/2.1.3263.3929.

Archibald, S., Lehmann, C. E. R., Gómez-Dans, J. L., and Bradstock, R. A. (2013). Defining pyromes and global syndromes of fire regimes. PNAS USA 110, 6442–6447. doi: 10.1073/pnas.1211466110.

Archibald, S., Lehmann, C. E. R., Belcher, C. M., Bond, W. J., Bradstock, R. A., Daniau, A.-L., et al. (2018). Biological and geophysical feedbacks with fire in the Earth system. Environ. Res. Lett. 13, 033003. doi: 10.1088/1748-9326/aa9ead.

Baisheva I., Pestryakova L., Levina S., Glückler R., Biskaborn B. K., Vyse S. A., et al. (2022). Permafrost thaw lake development in Central Yakutia during the Holocene from sediment element composition and ancient DNA records. [In prep.].

https://doi.org/10.5194/egusphere-2022-395
Preprint. Discussion started: 25 May 2022

Barhoumi, C., Ali, A., Peyron, O., Dugerdil, L., Borisova, O., Golubeva, Y., et al. (2020). Did long-term fire control the coniferous boreal forest composition of the northern Ural region (Komi Republic, Russia)? J. Biogeogr. 47, 2426–2441. doi: 10.1111/jbi.13922.

Barhoumi, C., Vogel, M., Dugerdil, L., Limani, H., Joannin, S., Peyron, O., et al. (2021). Holocene fire regime changes in the southern Lake Baikal region influenced by climate-vegetation-anthropogenic activity interactions. Forests 12, 978. doi: 10.3390/f12080978.

Bennett, K. D. (1996). Determination of the number of zones in a biostratigraphical sequence. New Phytol. 132, 155–170. doi: 10.1111/j.1469-8137.1996.tb04521.x.

Biskaborn, B. K., Herzschuh, U., Bolshiyanov, D., Savelieva, L., and Diekmann, B. (2012). Environmental variability in northeastern Siberia during the last ~13,300yr inferred from lake diatoms and sediment–geochemical parameters. Palaeogeogr. Palaeoclimatol., Palaeoecol. 329–330, 22–36. doi: 10.1016/j.palaeo.2012.02.003.

Blaauw, M., and Christen, J. A. (2011). Flexible paleoclimate age-depth models using an autoregressive gamma process. Bayesian Anal. 6, 457–474. doi: 10.1214/11-BA618.

Blaauw, M., Christen, A., and Aquino L., M. A. (2021): rbacon: Age-Depth Modelling using Bayesian Statistics. R package version 2.5.7. Available at: https://CRAN.R-project.org/package=rbacon [Accessed March 10, 2022].

Boike, J., Grau, T., Heim, B., Günther, F., Langer, M., Muster, S., et al. (2016). Satellite-derived changes in the permafrost landscape of central Yakutia, 2000–2011: Wetting, drying, and fires. Glob. Planet. Change 139, 116–127. doi: 10.1016/j.gloplacha.2016.01.001.

Bowman, D. M. J. S., Kolden, C. A., Abatzoglou, J. T., Johnston, F. H., van der Werf, G. R., and Flannigan, M. (2020). Vegetation fires in the Anthropocene. Nat. Rev. Earth Environ. 1, 500–515. doi: 10.1038/s43017-020-0085-3.

Boyer, F., Mercier, C., Bonin, A., Le Bras, Y., Taberlet, P., and Coissac, E. (2016). obitools: a unix-inspired software package for DNA metabarcoding. Mol. Ecol. Resour. 16, 176–182. doi: 10.1111/1755-0998.12428.

Bulygina, O. N., Razuvaev, V. N., and Korshunova, N. N. (2009). Changes in snow cover over Northern Eurasia in the last few decades. Environ. Res. Lett. 4, 045026. doi: 10.1088/1748-9326/4/4/045026.

Cao, X., Tian, F., Dallmeyer, A., and Herzschuh, U. (2019a). Northern Hemisphere biome changes (>30°N) since 40 cal ka BP and their driving factors inferred from model-data comparisons. Quat. Sci. Rev. 220, 291–309. doi: 10.1016/j.quascirev.2019.07.034.

https://doi.org/10.5194/egusphere-2022-395
Preprint. Discussion started: 25 May 2022

Cao, X., Tian, F., Li, F., Gaillard, M.-J., Rudaya, N., Xu, Q., et al. (2019b). Pollen-based quantitative land-cover reconstruction for northern Asia covering the last 40 ka cal BP. Clim. Past 15, 1503–1536. doi: 10.5194/cp-15-1503-2019.

Chytrý, M., Danihelka, J., Kubešová, S., Lustyk, P., Ermakov, N., Hájek, M., et al. (2008). Diversity of forest vegetation across a strong gradient of climatic continentality: Western Sayan Mountains, southern Siberia. Plant Ecol. 196, 61–83. doi: 10.1007/s11258-007-9335-4.

Clark, J. S. (1988). Particle motion and the theory of charcoal analysis: Source area, transport, deposition, and sampling. Quat. Res. 30, 67–80. doi: 10.1016/0033-5894(88)90088-9.

Coffman, G. C., Ambrose, R. F., and Rundel, P. W. (2010). Wildfire promotes dominance of invasive giant reed (*Arundo donax*) in riparian ecosystems. Biol. Invasions 12, 2723–2734. doi: 10.1007/s10530-009-9677-z.

Colman, S. M., Jones, G. A., Rubin, M., King, J. W., Peck, J. A., and Orem, W. H. (1996). AMS radiocarbon analyses from Lake Baikal, Siberia: Challenges of dating sediments from a large, oligotrophic lake. Quat. Sci. Rev. 15, 669–684. doi: 10.1016/0277-3791(96)00027-3.

Conedera, M., Tinner, W., Neff, C., Meurer, M., Dickens, A. F., and Krebs, P. (2009). Reconstructing past fire regimes: methods, applications, and relevance to fire management and conservation. Quat. Sci. Rev. 28, 555–576. doi: 10.1016/j.quascirev.2008.11.005.

Constantine, M., and Mooney, S. (2021). Widely used charcoal analysis method in paleo studies involving NaOCl results in loss of charcoal formed below 400°C. Holocene, 09596836211041740. doi: 10.1177/09596836211041740.

Courtin, J., Andreev, A. A., Raschke, E., Bala, S., Biskaborn, B. K., Liu, S., et al. (2021). Vegetation changes in southeastern Siberia during the Late Pleistocene and the Holocene. Front. Ecol. Evol. 9, 625096. doi: 10.3389/fevo.2021.625096.

Crate, S., Ulrich, M., Habeck, J. O., Desyatkin, A. R., Desyatkin, R. V., Fedorov, A. N., et al. (2017). Permafrost livelihoods: A transdisciplinary review and analysis of thermokarst-based systems of indigenous land use. Anthropocene 18, 89–104. doi: 10.1016/j.ancene.2017.06.001.

Deluca, T. H., and Boisvenue, C. (2012). Boreal forest soil carbon: distribution, function and modelling. Forestry 85, 161–184. doi: 10.1093/forestry/cps003.

Dietze, E., Brykała, D., Schreuder, L. T., Jażdżewski, K., Blarquez, O., Brauer, A., et al. (2019). Human-induced fire regime shifts during 19th century industrialization: A robust fire regime reconstruction using northern Polish lake sediments. PLOS ONE 14, e0222011. doi: 10.1371/journal.pone.0222011.

https://doi.org/10.5194/egusphere-2022-395
Preprint. Discussion started: 25 May 2022

Dietze, E., Mangelsdorf, K., Andreev, A., Karger, C., Schreuder, L. T., Hopmans, E. C., et al. (2020). Relationships between low-temperature fires, climate and vegetation during three late glacials and interglacials of the last 430kyr in northeastern Siberia reconstructed from monosaccharide anhydrides in Lake El'gygytgyn sediments. Clim. Past 16, 799–818. doi: 10.5194/cp-16-799-2020.

Ding, Y., Yamashita, Y., Jones, J., and Jaffé, R. (2015). Dissolved black carbon in boreal forest and glacial rivers of central Alaska: assessment of biomass burning versus anthropogenic sources. Biogeochemistry 123, 15–25. doi: 10.1007/s10533-014-0050-7.

Dryad Digital Repository. Available at: https://datadryad.org/stash [Accessed May 22, 2022]

Edwards, M. E., Anderson, P. M., Brubaker, L. B., Ager, T. A., Andreev, A. A., Bigelow, N. H., et al. (2000). Pollen-based biomes for Beringia 18,000, 6000 and 0 14C yr BP. J. Biogeogr. 27, 521–554. doi: 10.1046/j.1365-2699.2000.00426.x.

Enache, M. D., and Cumming, B. F. (2006). Tracking recorded fires using charcoal morphology from the sedimentary sequence of Prosser Lake, British Columbia (Canada). Quat. Res. 65, 282–292. doi: 10.1016/j.yqres.2005.09.003.

Enache, M. D., and Cumming, B. F. (2007). Charcoal morphotypes in lake sediments from British Columbia (Canada): an assessment of their utility for the reconstruction of past fire and precipitation. J. Paleolimnol. 38, 347–363. doi: 10.1007/s10933-006-9084-8.

Fedorov, A. N., Konstantinov, P. Y., Vasilyev, N. F., and Shestakova, A. A. (2019). The influence of boreal forest dynamics on the current state of permafrost in Central Yakutia. Polar Sci. 22, 100483. doi: 10.1016/j.polar.2019.100483.

Feurdean, A. (2021). Experimental production of charcoal morphologies to discriminate fuel source and fire type: an example from Siberian taiga. Biogeosciences 18, 3805–3821. doi: 10.5194/bg-18-3805-2021.

Feurdean, A., Diaconu, A.-C., Pfeiffer, M., Gałka, M., Hutchinson, S. M., Butiseaca, G., et al. (2021). Holocene wildfire regimes in forested peatlands in western Siberia: interaction between peatland moisture conditions and the composition of plant functional types. Clim. Past Discussions [Accepted]. Available at: doi: 10.5194/cp-2021-125 (Accessed May 05, 2022).

Finsinger, W., and Tinner, W. (2005). Minimum count sums for charcoal concentration estimates in pollen slides: accuracy and potential errors. Holocene 15, 293–297. doi: 10.1191/0959683605hl808rr.

Geng R., Andreev A., Kruse S., Heim B., van Geffen F., Pestryakova L., et al. (2022). Modern pollen assemblages from lake sediments and soil in East Siberia and relative pollen productivity estimates for major taxa. Front. Ecol. Evol. [Accepted]. Available at: https://www.frontiersin.org/articles/10.3389/fevo.2022.837857/abstract (Accessed May 24, 2022).

https://doi.org/10.5194/egusphere-2022-395
Preprint. Discussion started: 25 May 2022

Giglio, L., Schroeder, W., and Justice, C. O. (2016). The collection 6 MODIS active fire detection algorithm and fire products. Remote Sens. Environ. 178, 31–41. doi: 10.1016/j.rse.2016.02.054.

Glew, J. R., Smol, J. P., and Last, W. M. (2002). "Sediment core collection and extrusion," in Tracking Environmental Change Using Lake Sediments Vol. 1: Basin Analysis, Coring, and Chronological Techniques, eds. W. M. Last and J. P. Smol (Dordrecht: Kluwer Academic Publishers), 73–105. doi: 10.1007/0-306-47669-X_5.

Glückler, R., Herzschuh, U., Kruse, S., Andreev, A., Vyse, S. A., Winkler, B., et al. (2021). Wildfire history of the boreal forest of south-western Yakutia (Siberia) over the last two millennia documented by a lake-sediment charcoal record. Biogeosciences 18, 4185–4209. doi: 10.5194/bg-18-4185-2021.

Grimm, E. C. (1987). CONISS: a FORTRAN 77 program for stratigraphically constrained cluster analysis by the method of incremental sum of squares. Comput. Geosci. 13, 13–35. doi: 10.1016/0098-3004(87)90022-7.

Harris, I., Osborn, T. J., Jones, P., and Lister, D. (2020). Version 4 of the CRU TS monthly high-resolution gridded multivariate climate dataset. Sci. Data 7, 109. doi: 10.1038/s41597-020-0453-3.

He, F. (2011). Simulating transient climate evolution of the last deglaciation with CCSM3. [PhD Dissertation]. [Madison (WI)]: University of Wisconsin-Madison

Hersbach, H., Bell, B., Berrisford, P., Hirahara, S., Horányi, A., Muñoz-Sabater, J., et al. (2020). The ERA5 global reanalysis. Q. J. R. Meteorol. Soc. 146, 1999–2049. doi: 10.1002/qj.3803.

Herzschuh, U. (2020). Legacy of the Last Glacial on the present-day distribution of deciduous versus evergreen boreal forests. Glob. Ecol. Biogeogr. 29, 198–206. doi: 10.1111/geb.13018.

Herzschuh, U., Birks, H. J. B., Laepple, T., Andreev, A., Melles, M., and Brigham-Grette, J. (2016). Glacial legacies on interglacial vegetation at the Pliocene-Pleistocene transition in NE Asia. Nat. Commun. 7, 11967. doi: 10.1038/ncomms11967.

Higuera, P. E., Brubaker, L. B., Anderson, P. M., Hu, F. S., and Brown, T. A. (2009). Vegetation mediated the impacts of postglacial climate change on fire regimes in the south-central Brooks Range, Alaska. Ecol. Monogr. 79, 201–219. doi: 10.1890/07-2019.1.

Higuera, P. E., Peters, M. E., Brubaker, L. B., and Gavin, D. G. (2007). Understanding the origin and analysis of sediment-charcoal records with a simulation model. Quat. Sci. Rev. 26, 1790–1809. doi: 10.1016/j.quascirev.2007.03.010.

https://doi.org/10.5194/egusphere-2022-395
Preprint. Discussion started: 25 May 2022

Holloway, J., Lewkowicz, A., Douglas, T., li, X., Turetsky, M., Baltzer, J., et al. (2020). Impact of wildfire on permafrost landscapes: A review of recent advances and future prospects. Permafr. Periglac. Process. 31. doi: 10.1002/ppp.2048.

Hood, S. M., Varner, J. M., van Mantgem, P., and Cansler, C. A. (2018). Fire and tree death: understanding and improving modeling of fire-induced tree mortality. Environ. Res. Lett. 13, 113004. doi: 10.1088/1748-9326/aae934.

Hudspith, V. A., Belcher, C. M., Kelly, R., and Hu, F. S. (2015). Charcoal reflectance reveals early Holocene boreal deciduous forests burned at high intensities. PLOS ONE 10, e0120835. doi: 10.1371/journal.pone.0120835.

International Paleofire Network: Global Paleofire Database. Available at: https://ipn.paleofire.org/ [Accessed May 12, 2022].

Isaev, A. P., Protopopov, A. V., Protopopova, V. V., Egorova, A. A., Timofeyev, P. A., Nikolaev, A. N., et al. (2010). "Vegetation of Yakutia: Elements of Ecology and Plant Sociology," in The Far North Plant and Vegetation., eds. E. I. Troeva, A. P. Isaev, M. M. Cherosov, and N. S. Karpov (Dordrecht: Springer Netherlands), 143–260. doi: 10.1007/978-90-481-3774-9_3.

Jensen, K., Lynch, E. A., Calcote, R., and Hotchkiss, S. C. (2007). Interpretation of charcoal morphotypes in sediments from Ferry Lake, Wisconsin, USA: do different plant fuel sources produce distinctive charcoal morphotypes? Holocene 17, 907–915. doi: 10.1177/0959683607082405.

Juggins, S. (2020). rioja: Analysis of Quaternary Science Data. R package version 0.9-26. Available at: https://cran.r-project.org/package=rioja [Accessed March 10, 2022].

Karp, A. T., Holman, A. I., Hopper, P., Grice, K., and Freeman, K. H. (2020). Fire distinguishers: Refined interpretations of polycyclic aromatic hydrocarbons for paleo-applications. Geochim. Cosmochim. Acta 289, 93–113. doi: 10.1016/j.gca.2020.08.024.

Katamura, F., Fukuda, M., Bosikov, N. P., and Desyatkin, R. V. (2009a). Charcoal records from thermokarst deposits in central Yakutia, eastern Siberia: Implications for forest fire history and thermokarst development. Quat. Res. 71, 36–40. doi: 10.1016/j.yqres.2008.08.003.

Katamura, F., Fukuda, M., Bosikov, N. P., and Desyatkin, R. V. (2009b). Forest fires and vegetation during the Holocene in central Yakutia, eastern Siberia. J. For. Res. 14, 30–36. doi: 10.1007/s10310-008-0099-z.

Katamura, F., Fukuda, M., Bosikov, N. P., Desyatkin, R. V., Nakamura, T., and Moriizumi, J. (2006). Thermokarst formation and vegetation dynamics inferred from a palynological study in Central Yakutia, Eastern Siberia, Russia. Arct. Antarct. Alp. Res. 38, 561–570. doi: 10.1657/1523-0430(2006)38[561:TFAVDI]2.0.CO;2.

https://doi.org/10.5194/egusphere-2022-395
Preprint. Discussion started: 25 May 2022

Keeley, J. E. (2009). Fire intensity, fire severity and burn severity: a brief review and suggested usage. Int. J. Wildland Fire 18, 116. doi: 10.1071/WF07049.

Kharuk, V. I., Im, S. T., Petrov, I. A., Dvinskaya, M. L., Shushpanov, A. S., and Golyukov, A. S. (2021). Climate-driven conifer mortality in Siberia. Glob. Ecol. Biogeogr. 30, 543–556. doi: 10.1111/geb.13243.

Kirillina, K., Shvetsov, E. G., Protopopova, V. V., Thiesmeyer, L., and Yan, W. (2020). Consideration of anthropogenic factors in boreal forest fire regime changes during rapid socio-economic development: case study of forestry districts with increasing burnt area in the Sakha Republic, Russia. Environ. Res. Lett. 15, 035009. doi: 10.1088/1748-9326/ab6c6e.

Köster, K., Aaltonen, H., Berninger, F., Heinonsalo, J., Köster, E., Ribeiro-Kumara, C., et al. (2021). Impacts of wildfire on soil microbiome in Boreal environments. Curr. Opin. Environ. Sci. Health 22, 100258. doi: 10.1016/j.coesh.2021.100258.

Kruse, S., Bolshiyanov, D., Grigoriev, M. N., Morgenstern, A., Pestryakova, L., Tsibizov, L., et al. (2019). Russian-German Cooperation: Expeditions to Siberia in 2018. Report of the Polar Marine Research Group, 734, 1–257. doi: 10.2312/BzPM_0734_2019.

Kruse, S., Farkas, L., Brieger, F., Geng, R., Heim, B., Pestryakova, L. A., et al. Data from: SiDroForest: Orthomosaics, SfM point clouds and products from aerial image data of expedition vegetation plots in 2018 in Central Yakutia and Chukotka, Siberia. PANGAEA. (2021) https://doi.pangaea.de/10.1594/PANGAEA.933263.

Kruse, S., Wieczorek, M., Jeltsch, F., and Herzschuh, U. (2016). Treeline dynamics in Siberia under changing climates as inferred from an individual-based model for *Larix*. Ecol. Model. 338, 101–121. doi: 10.1016/j.ecolmodel.2016.08.003.

Kukavskaya, E. A., Buryak, L. V., Ivanova, G. A., Conard, S. G., Kalenskaya, O. P., Zhila, S. V., et al. (2013). Influence of logging on the effects of wildfire in Siberia. Environ. Res. Lett. 8, 045034. doi: 10.1088/1748-9326/8/4/045034.

Lasslop, G., Brovkin, V., Reick, C. H., Bathiany, S., and Kloster, S. (2016). Multiple stable states of tree cover in a global land surface model due to a fire-vegetation feedback. Geophys. Res. Lett. 43, 6324–6331. doi: 10.1002/2016GL069365.

Lenton, T. M. (2012). Arctic climate tipping points. Ambio 41, 10–22. doi:10.1007/s13280-011-0221-x.

Leys, B. A., Commerford, J. L., and McLauchlan, K. K. (2017). Reconstructing grassland fire history using sedimentary charcoal: Considering count, size and shape. PLOS ONE 12, e0176445. doi: 10.1371/journal.pone.0176445.

https://doi.org/10.5194/egusphere-2022-395
Preprint. Discussion started: 25 May 2022

Liu, S., Stoof-Leichsenring, K. R., Kruse, S., Pestryakova, L. A., and Herzschuh, U. (2020). Holocene vegetation and plant diversity changes in the north-eastern Siberian treeline region from pollen and sedimentary ancient DNA. Front. Ecol. Evol. 8, 560243. doi: 10.3389/fevo.2020.560243.

Maezumi, S. Y., Gosling, W. D., Kirschner, J., Chevalier, M., Cornelissen, H. L., Heinecke, T., et al. (2021). A modern analogue matching approach to characterize fire temperatures and plant species from charcoal. Palaeogeogr. Palaeoclimatol. Palaeoecol. 578, 110580. doi: 10.1016/j.palaeo.2021.110580.

Ministry for Natural Resources and Ecology of the Russian Federation (2012). Geological Map of Russia and Adjoining Water Areas, Scale 1:2,500,000. Available at: https://www.vsegei.ru/ru/info/gk-2500/index.php [Accessed March 10, 2022].

Ministry for Natural Resources and Ecology of the Russian Federation (2014). Map of the Quaternary Formations of the Russian Federation, Scale 1:2,500,000. Available at: https://vsegei.ru/ru/info/quaternary-2500/ [Accessed March 10, 2022].

Mollenhauer, G., Grotheer, H., Gentz, T., Bonk, E., and Hefter, J. (2021). Standard operation procedures and performance of the MICADAS radiocarbon laboratory at Alfred Wegener Institute (AWI), Germany. Nucl. Instrum. Methods Phys. Res. B: Beam Interact. Mater. At. 496, 45–51. doi: 10.1016/j.nimb.2021.03.016.

Müller, S., Tarasov, P. E., Andreev, A. A., and Diekmann, B. (2009). Late Glacial to Holocene environments in the present-day coldest region of the Northern Hemisphere inferred from a pollen record of Lake Billyakh, Verkhoyansk Mts, NE Siberia. Clim. Past 5, 73–84. doi: 10.5194/cp-5-73-2009.

Mustaphi, C. J. C., and Pisaric, M. F. J. (2014). A classification for macroscopic charcoal morphologies found in Holocene lacustrine sediments. Prog. Phys. Geogr. 38, 734–754. doi: 10.1177/0309133314548886.

Narita, D., Gavrilyeva, T., and Isaev, A. (2021). Impacts and management of forest fires in the Republic of Sakha, Russia: A local perspective for a global problem. Polar Sci. 27, 100573. doi: 10.1016/j.polar.2020.100573.

Nakane, M., Ajioka, T., and Yamashita, Y. (2017). Distribution and sources of dissolved black carbon in surface waters of the Chukchi Sea, Bering Sea, and the North Pacific Ocean. Front. Earth Sci. 5, 34. doi: 10.3389/feart.2017.00034.

Oksanen, J., Blanchet, F. G., Friendly, M., Kindt, R., Legendre, P., McGlinn, D, et al. (2020). vegan: Community Ecology Package. R package version 2.5-7. Available at: https://CRAN.R-project.org/package=vegan [Accessed March 10, 2022].

PANGAEA. Data Publisher for Earth & Environmental Science. Available at: https://pangaea.de/ [Accessed May 12, 2022].

Philippsen, B. (2013). The freshwater reservoir effect in radiocarbon dating. Herit. Sci. 1, 24. doi: 10.1186/2050-7445-1-24.

https://doi.org/10.5194/egusphere-2022-395
Preprint. Discussion started: 25 May 2022

Ponomarev, E. I., Shvetsov, E. G., and Kharuk, V. I. (2018). The intensity of wildfires in fire emissions estimates. Russ. J. Ecol. 49, 492–499. doi: 10.1134/S1067413618060097.

Ponomarev, E., Yakimov, N., Ponomareva, T., Yakubailik, O., and Conard, S. G. (2021). Current trend of carbon emissions from wildfires in Siberia. Atmosphere 12, 559. doi: 10.3390/atmos12050559.

Power, M. J., Marlon, J. R., Bartlein, P. J., and Harrison, S. P. (2010). Fire history and the Global Charcoal Database: A new tool for hypothesis testing and data exploration. Palaeogeogr. Palaeoclimatol. Palaeoecol. 291, 52–59. doi: 10.1016/j.palaeo.2009.09.014.

R Core Team (2020). R: A language and environment for statistical computing. R Foundation for Statistical Computing, Vienna, Austria. Available at: https://www.R-project.org/ [Accessed March 10, 2022].

Reimer, P. J., Austin, W. E. N., Bard, E., Bayliss, A., Blackwell, P. G., Ramsey, C. B., et al. (2020). The IntCal20 Northern Hemisphere radiocarbon age calibration curve (0–55 cal kBP). Radiocarbon 62, 725–757. doi: 10.1017/RDC.2020.41.

Reyer, C. P. O., Brouwers, N., Rammig, A., Brook, B. W., Epila, J., Grant, R. F., et al. (2015). Forest resilience and tipping points at different spatio-temporal scales: approaches and challenges. J. Ecol. 103, 5–15. doi: 10.1111/1365-2745.12337.

Reza, M. S., Afroze, S., Bakar, M. S. A., Saidur, R., Aslfattahi, N., Taweekun, J., et al. (2020). Biochar characterization of invasive *Pennisetum purpureum* grass: effect of pyrolysis temperature. Biochar 2, 239–251. doi: 10.1007/s42773-020-00048-0.

Rogers, B. M., Soja, A. J., Goulden, M. L., and Randerson, J. T. (2015). Influence of tree species on continental differences in boreal fires and climate feedbacks. Nat. Geosci. 8, 228–234. doi: 10.1038/ngeo2352.

Scheffer, M., Hirota, M., Holmgren, M., Van Nes, E. H., and Chapin, F. S. (2012). Thresholds for boreal biome transitions. PNAS USA. 109, 21384–21389. doi: 10.1073/pnas.1219844110.

Shuman, J. K., Foster, A. C., Shugart, H. H., Hoffman-Hall, A., Krylov, A., Loboda, T., et al. (2017). Fire disturbance and climate change: implications for Russian forests. Environ. Res. Lett. 12, 035003. doi: 10.1088/1748-9326/aa5eed.

Soininen, E. M., Gauthier, G., Bilodeau, F., Berteaux, D., Gielly, L., Taberlet, P., et al. (2015). Highly overlapping winter diet in two sympatric lemming species revealed by DNA metabarcoding. PLOS ONE 10, e0115335. doi: 10.1371/journal.pone.0115335.

https://doi.org/10.5194/egusphere-2022-395
Preprint. Discussion started: 25 May 2022

Sønstebø, J. H., Gielly, L., Brysting, A. K., Elven, R., Edwards, M., Haile, J., et al. (2010). Using next-generation sequencing for molecular reconstruction of past Arctic vegetation and climate. Mol. Ecol. Resour. 10, 1009–1018. doi: 10.1111/j.1755-0998.2010.02855.x.

Stocks, B. J., Lawson, B. D., Alexander, M. E., Wagner, C. E. V., McAlpine, R. S., Lynham, T. J., et al. (1989). The Canadian Forest Fire Danger Rating System: An overview. For. Chron. 65, 450–457. doi: 10.5558/tfc65450-6.

Stoof-Leichsenring, K. R., Epp, L. S., Trauth, M. H., and Tiedemann, R. (2012). Hidden diversity in diatoms of Kenyan Lake Naivasha: a genetic approach detects temporal variation. Mol. Ecol. 21, 1918–1930. doi: 10.1111/j.1365-294X.2011.05412.x.

Stuenzi, S. M., Boike, J., Cable, W., Herzschuh, U., Kruse, S., Pestryakova, L. A., et al. (2021). Variability of the surface energy balance in permafrost-underlain boreal forest. Biogeosciences 18, 343–365. doi: 10.5194/bg-18-343-2021.

Sugita, S. (2007). Theory of quantitative reconstruction of vegetation I: pollen from large sites REVEALS regional vegetation composition. Holocene 17, 229–241. doi: 10.1177/0959683607075837.

Taberlet, P., Coissac, E., Pompanon, F., Gielly, L., Miquel, C., Valentini, A., et al. (2007). Power and limitations of the chloroplast trnL (UAA) intron for plant DNA barcoding. Nucleic Acids Res. 35, e14–e14. doi: 10.1093/nar/gkl938.

Tei, S., Sugimoto, A., Yonenobu, H., Kotani, A., and Maximov, T. C. (2019). Effects of extreme drought and wet events for tree mortality: Insights from tree-ring width and carbon isotope ratio in a Siberian larch forest. Ecohydrology 12, e2143. doi: 10.1002/eco.2143.

Theuerkauf, M., Couwenberg, J., Kuparinen, A., and Liebscher, V. (2016). A matter of dispersal: REVEALSinR introduces state-of-the-art dispersal models to quantitative vegetation reconstruction. Veg. Hist. Archaeobotany 25, 541–553. doi: 10.1007/s00334-016-0572-0.

Tsuyuzaki, S., Iwahana, G., and Saito, K. (2018). Tundra fire alters vegetation patterns more than the resultant thermokarst. Polar Biol. 41, 753–761. doi: 10.1007/s00300-017-2236-7.

Ulrich, M., Matthes, H., Schmidt, J., Fedorov, A. N., Schirrmeister, L., Siegert, C., et al. (2019). Holocene thermokarst dynamics in Central Yakutia – A multi-core and robust grain-size endmember modeling approach. Quat. Sci. Rev. 218, 10–33. doi: 10.1016/j.quascirev.2019.06.010.

Vachula, R. S., and Richter, N. (2018). Informing sedimentary charcoal-based fire reconstructions with a kinematic transport model. Holocene 28, 173–178. doi: 10.1177/0959683617715624.

https://doi.org/10.5194/egusphere-2022-395
Preprint. Discussion started: 25 May 2022

Vachula, R. S., Sae-Lim, J., and Li, R. (2021). A critical appraisal of charcoal morphometry as a paleofire fuel type proxy. Quat. Sci. Rev. 262, 106979. doi: 10.1016/j.quascirev.2021.106979.

van den Boogaart, K. G., Tolosana-Delgado, R., and Bren, M. (2021). compositions: Compositional Data Analysis. R package version 2.0-2. Available at: https://CRAN.R-project.org/package=compositions [Accessed March 10, 2022].

van Geffen, F., Heim, B., Brieger, F., Geng, R., Shevtsova, I. A., Schulte, L., et al. (2021). SiDroForest: A comprehensive forest inventory of Siberian boreal forest investigations including drone-based point clouds, individually labelled trees, synthetically generated tree crowns and Sentinel-2 labelled image patches. Earth Syst. Sci. Data Discussions, 1–44 [Preprint]. Available at: doi: 10.5194/essd-2021-281 (Accessed May 22, 2022).

Velichko, A. A., Andreev, A. A., and Klimanov, V. A. (1997). Climate and vegetation dynamics in the tundra and forest zone during the late glacial and Holocene. Quat. Int. 41–42, 71–96. doi: 10.1016/S1040-6182(96)00039-0.

Voiland, A. (2021). An Unusually Smoky Fire Season in Sakha. NASA Earth Observatory. Available at: https://earthobservatory.nasa.gov/images/148678/an-unusually-smoky-fire-season-in-sakha [Accessed February 24, 2022].

Vyse, S. A., Herzschuh, U., Andreev, A. A., Pestryakova, L. A., Diekmann, B., Armitage, S. J., et al. (2020). Geochemical and sedimentological responses of arctic glacial Lake Ilirney, Chukotka (far east Russia) to palaeoenvironmental change since ~51.8 ka BP. Quat. Sci. Rev. 247, 106607. doi: 10.1016/j.quascirev.2020.106607.

Walker, X. J., Baltzer, J. L., Cumming, S. G., Day, N. J., Ebert, C., Goetz, S., et al. (2019). Increasing wildfires threaten historic carbon sink of boreal forest soils. Nature 572, 520–523. doi: 10.1038/s41586-019-1474-y.

Walter, K. M., Edwards, M. E., Grosse, G., Zimov, S. A., and Chapin, F. S. (2007). Thermokarst lakes as a source of atmospheric CH_4 during the last deglaciation. Science 318, 633–636. doi: 10.1126/science.1142924.

Wang, X., Wotton, B. M., Cantin, A. S., Parisien, M.-A., Anderson, K., Moore, B., et al. (2017). cffdrs: an R package for the Canadian Forest Fire Danger Rating System. Ecol. Process. 6, 5. doi: 10.1186/s13717-017-0070-z.

Ward, D. E., and Hardy, C. C. (1991). Smoke emissions from wildland fires. Environ. Int. 17, 117–134.

Whitlock, C., and Anderson, R. S. (2003). "Fire history reconstructions based on sediment records from lakes and wetlands," in Fire and Climatic Change in Temperate Ecosystems of the Western Americas Ecological Studies., eds. T. T. Veblen, W. L. Baker, G. Montenegro, and T. W. Swetnam (New York: Springer-Verlag), 3–31. doi: 10.1007/0-387-21710-X_1.

https://doi.org/10.5194/egusphere-2022-395
Preprint. Discussion started: 25 May 2022

Whitlock, C., and Larsen, C. (2001). "Charcoal as a fire proxy," in Tracking Environmental Change Using Lake Sediments, Vol. 3: Terrestrial, Algal, and Siliceous Indicators, eds. J. P. Smol, H. J. B. Birks, and W. M. Last (Dordrecht: Springer Netherlands), 75–97. doi: 10.1007/0-306-47668-1_5.

Wieczorek, M., and Herzschuh, U. (2020). Compilation of relative pollen productivity (RPP) estimates and taxonomically harmonised RPP datasets for single continents and Northern Hemisphere extratropics. Earth Syst. Sci. Data 12, 3515–3528. doi: 10.5194/essd-12-3515-2020.

Willerslev, E., Davison, J., Moora, M., Zobel, M., Coissac, E., Edwards, M. E., et al. (2014). Fifty thousand years of Arctic vegetation and megafaunal diet. Nature 506, 47–51. doi: 10.1038/nature12921.

Wirth, C. (2005). "Fire regime and tree diversity in boreal forests: implications for the carbon cycle," in Forest Diversity and Function: Temperate and Boreal Systems Ecological Studies., eds. M. Scherer-Lorenzen, C. Körner, and E.-D. Schulze (Berlin, Heidelberg: Springer), 309–344. doi: 10.1007/3-540-26599-6_15.

Wragg, P. D., Mielke, T., and Tilman, D. (2018). Forbs, grasses, and grassland fire behaviour. J. Ecol. 106, 1983–2001. doi: 10.1111/1365-2745.12980.

Xu, W., Scholten, R. C., Hessilt, T. D., Liu, Y., and Veraverbeke, S. (2022). Overwintering fires rising in eastern Siberia. Environ. Res. Lett. 17, 045005. doi: 10.1088/1748-9326/ac59aa.

https://doi.org/10.5194/egusphere-2022-395
Preprint. Discussion started: 25 May 2022

Tables and figures

Table 1: ^{14}C dating results for sediment core EN18224-4. Samples marked with an * are considered outliers and excluded from the age-depth model.

Lab-ID	Depth (cm)	$F^{14}C \pm 1\sigma$	^{14}C yrs BP $\pm 1\sigma$	cal. yrs BP $\pm 2\sigma$
6172.1.1*	0-1	0.8326 ± 0.0021	1472 ± 21	1345.5 ± 36.5
6173.1.1	13-14	0.8121 ± 0.0021	1672 ± 21	1601.5 ± 73.5
6174.1.1	23-24	0.6782 ± 0.0018	3120 ± 21	3289 ± 36
6175.1.1	33-34	0.5998 ± 0.0016	4107 ± 22	4598 ± 73
6176.1.1	43-44	0.5789 ± 0.0016	4391 ± 22	4935 ± 67
6177.1.1	53-54	0.5749 ± 0.0016	4447 ± 22	5032 ± 69
6178.1.1	68-69	0.4758 ± 0.0013	5966 ± 23	6799 ± 63
6179.1.1	83-84	0.3862 ± 0.0011	7642 ± 24	8438 ± 58
6181.1.1	94-95	0.3504 ± 0.0011	8424 ± 24	9376.5 ± 43.5
6180.1.1	102-103	0.3274 ± 0.0010	8970 ± 25	9946 ± 15

https://doi.org/10.5194/egusphere-2022-395
Preprint. Discussion started: 25 May 2022

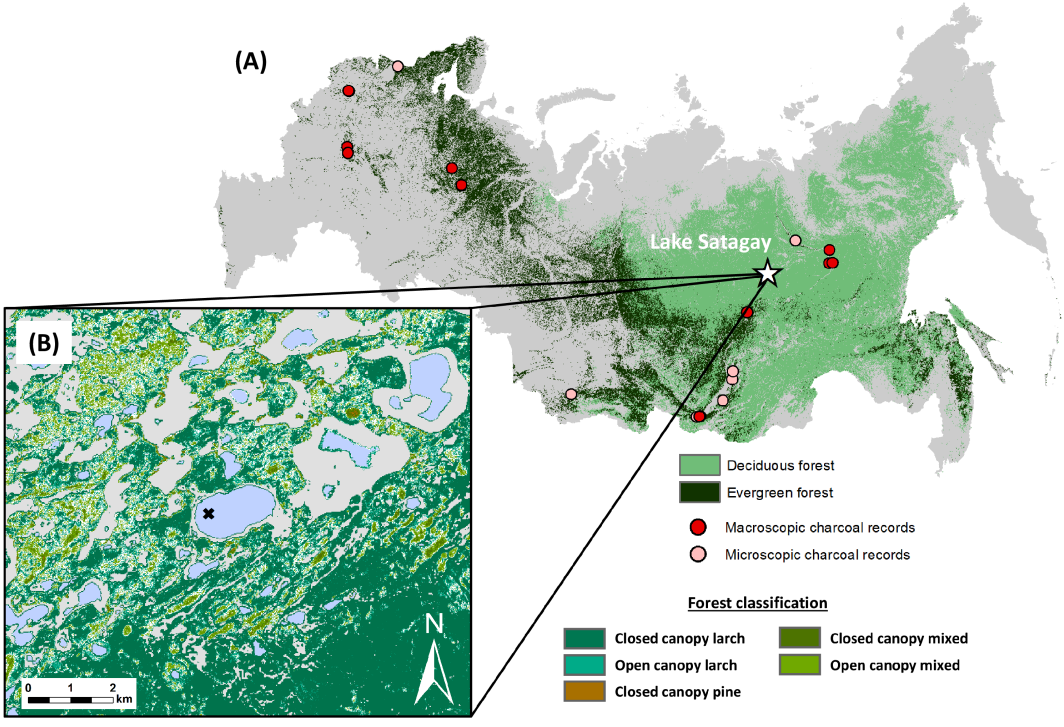

Figure 1 (A): Location of Lake Satagay (evergreen/deciduous forest classification based on © ESA Climate Change Initiative land cover project, provided via the Centre for Environmental Data Analysis (CEDA)). Red dots mark available sedimentary charcoal data from previous studies (extracted from the Global Paleofire Database and including only sites where data were provided, last access: 15 January 2022; Power et al., 2010). (B): Lake Satagay and its surrounding vegetation, based on land cover classification from Sentinel 2 acquisitions with ground truthing from expedition observations (Kruse et al., 2021; van Geffen et al., 2021[Preprint]; Geng et al., 2022[Accepted]).

https://doi.org/10.5194/egusphere-2022-395
Preprint. Discussion started: 25 May 2022

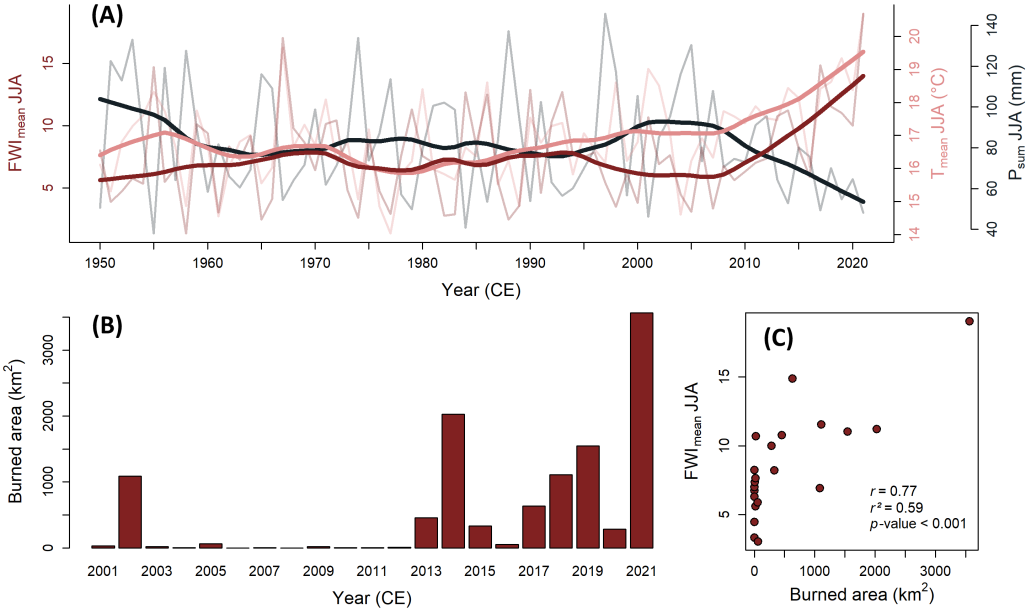

Figure 2 (A): ERA5 reanalysis data at Lake Satagay (Hersbach et al., 2020) for temperature, precipitation, and a fire-weather-index (FWI; calculated from daily values with the R package "cffdrs"; Wang et al., 2017) from 1950-2020 CE. (B): Burnt area in a 200 km buffer around Lake Satagay from 2001-2020 CE (NASA EOSDIS Land Processes DAAC product MCD64A1.006; Giglio et al., 2016). (C): Correlation of mean summer months FWI and annual burnt area.

https://doi.org/10.5194/egusphere-2022-395
Preprint. Discussion started: 25 May 2022

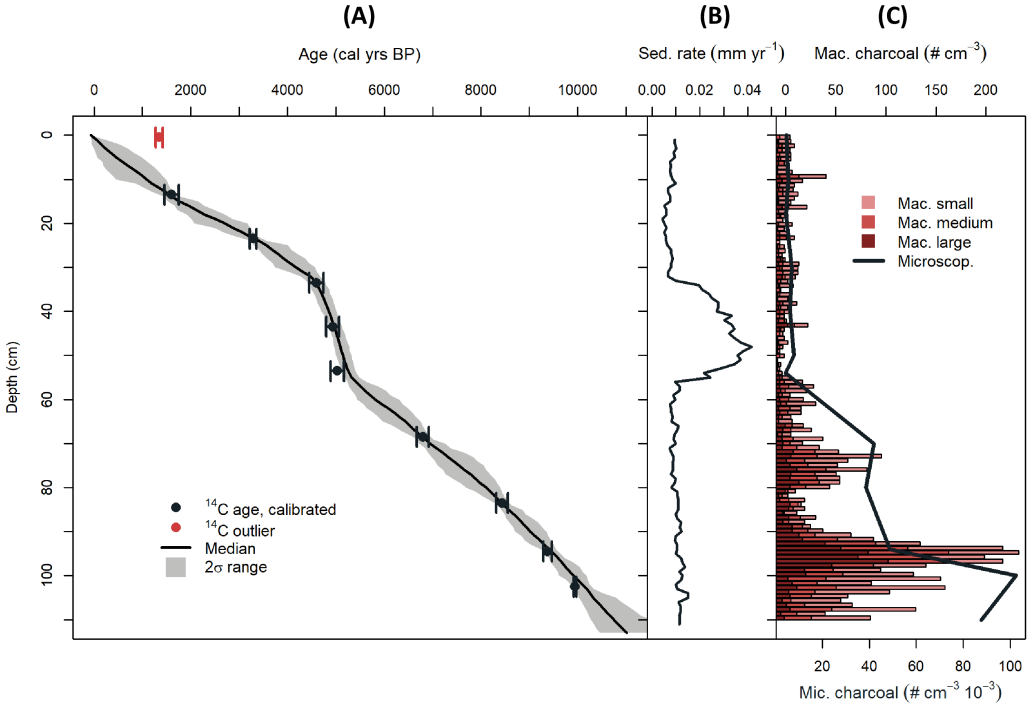

835 **Figure 3 (A): Bulk-sediment ^{14}C-based chronology for sediment core EN18224-4. (B): Sedimentation rate, as derived from the chronology. (C): Concentrations of macroscopic charcoal, divided by size classes (bars), and microscopic charcoal found in pollen samples (line).**

https://doi.org/10.5194/egusphere-2022-395
Preprint. Discussion started: 25 May 2022

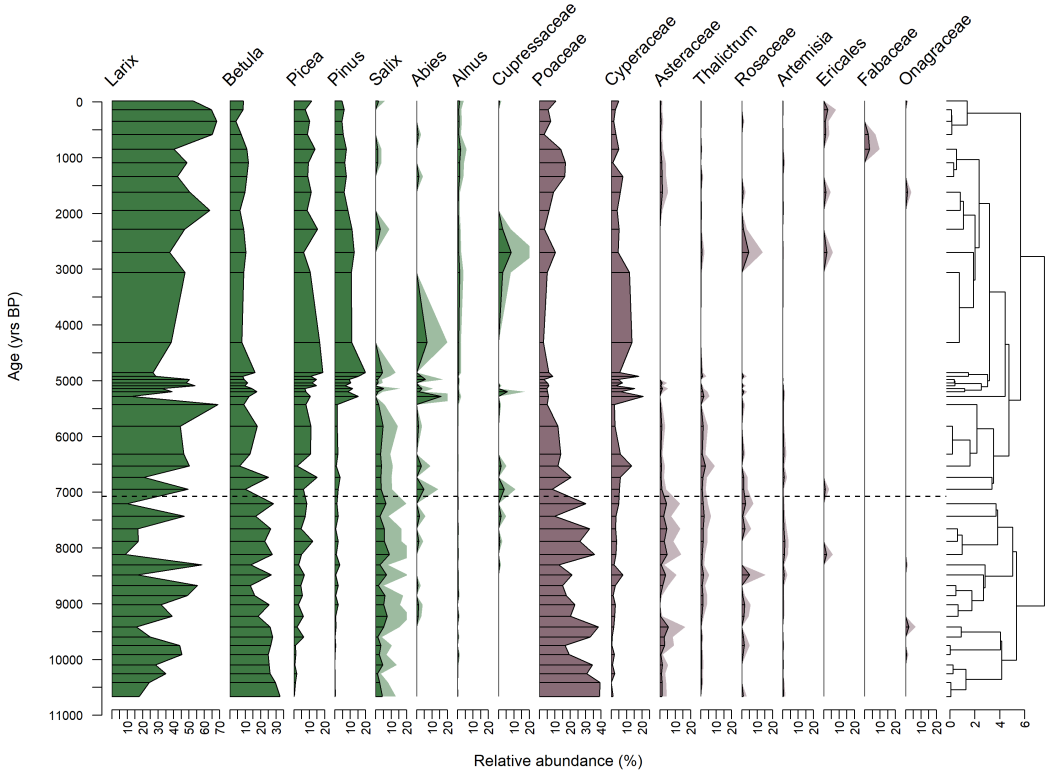

Figure 4: REVEALS-transformed pollen record, with zone separations from cluster analysis. Shaded area represents a visual exaggeration, added to pollen types of lower abundance.

https://doi.org/10.5194/egusphere-2022-395
Preprint. Discussion started: 25 May 2022

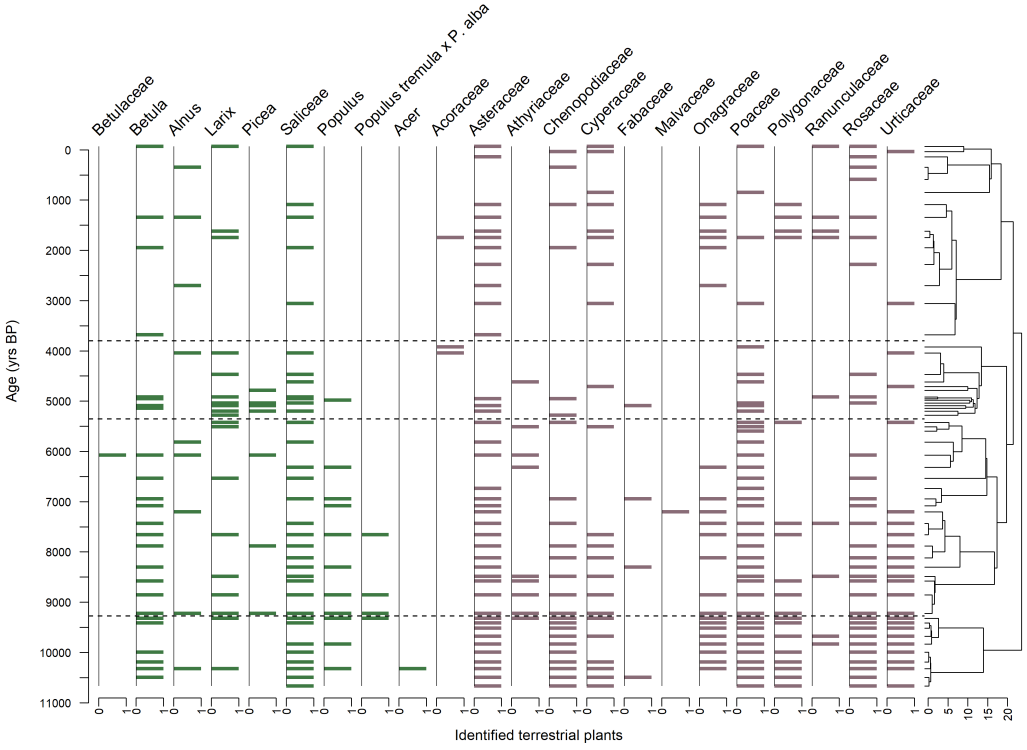

Figure 5: Sedimentary ancient DNA (sedaDNA) record for terrestrial plants, with zone separations from cluster analysis and displaying the presence or absence of plant types. Typical arboreal families are resolved to show the highest taxonomic level identified, whereas non-arboreal plants are shown on family level.

https://doi.org/10.5194/egusphere-2022-395
Preprint. Discussion started: 25 May 2022

Figure 6: (A) Photos of a low-severity surface fire plume and its impact near Nyurba and Lake Satagay in August 2019 (S. Stünzi and E. Dietze, AWI). (B) Photos of a high-severity fire plume and its impact near Ytyk-Kyuyol (c. 200 km east of Yakutsk) in August 2021 (R. Jackisch and R. Glückler, AWI).

https://doi.org/10.5194/egusphere-2022-395
Preprint. Discussion started: 25 May 2022

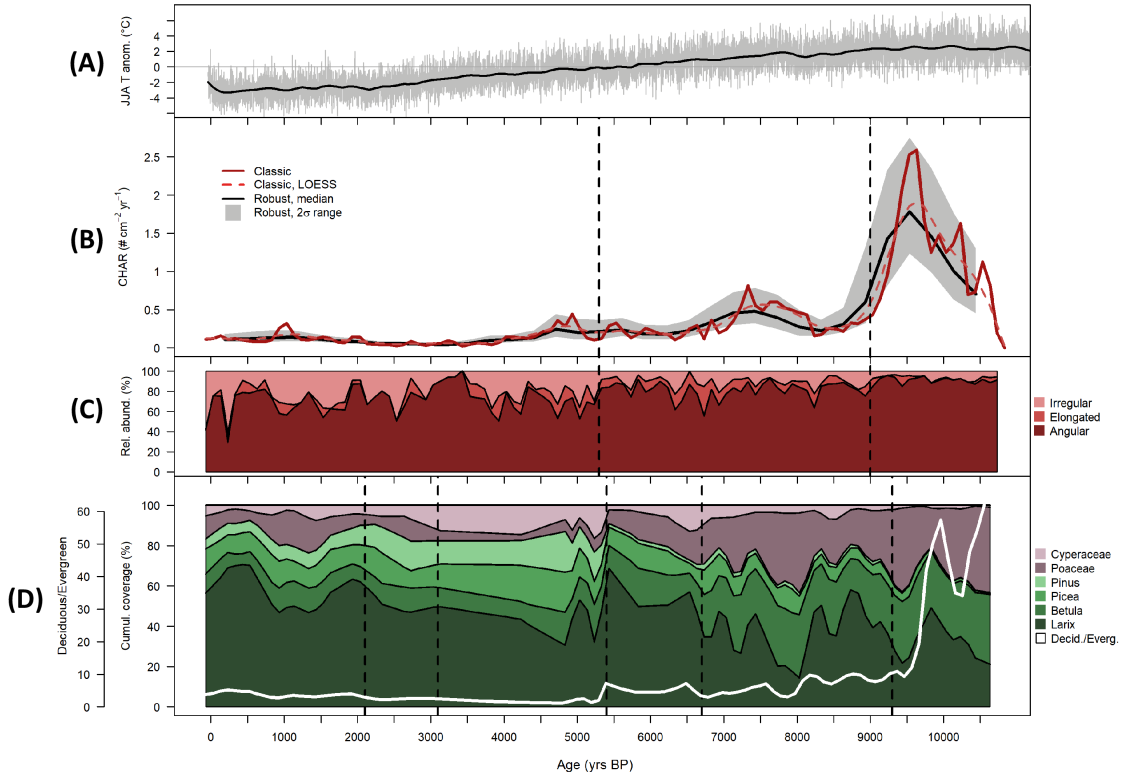

Figure 7: (A): TraCE 21ka climate model data (He, 2011) for Lake Satagay, displayed as annual June-August (JJA) temperature anomaly. (B): Classic and robust charcoal accumulation rates (CHAR), with zone separations from cluster analysis. (C): Relative abundance of charcoal morphotype classes, with zone separations from cluster analysis. (D): Cover of the most prominent vegetation types from the REVEALS-transformed pollen data, interpolated to match the median temporal resolution of the displayed charcoal data and with zone separations from cluster analysis (applied to interpolated data).

https://doi.org/10.5194/egusphere-2022-395
Preprint. Discussion started: 25 May 2022

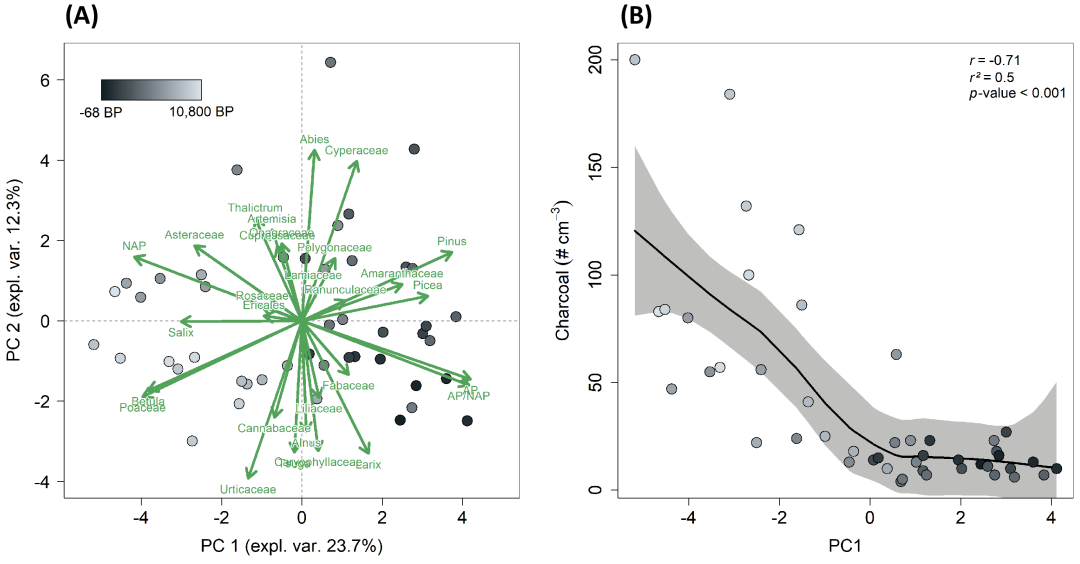

860

Figure 8: (A): PCA of REVEALS-transformed vegetation types. (B): Scatterplot of macroscopic charcoal concentration and principal component 1 (PC1) of the PCA, with LOESS-smoothing.